General Disclaimer

One or more of the Following Statements may affect this Document

- This document has been reproduced from the best copy furnished by the organizational source. It is being released in the interest of making available as much information as possible.

- This document may contain data, which exceeds the sheet parameters. It was furnished in this condition by the organizational source and is the best copy available.

- This document may contain tone-on-tone or color graphs, charts and/or pictures, which have been reproduced in black and white.

- This document is paginated as submitted by the original source.

- Portions of this document are not fully legible due to the historical nature of some of the material. However, it is the best reproduction available from the original submission.

Produced by the NASA Center for Aerospace Information (CASI)

(NASA-CR-141896) STUDIES OF RECOGNITION WITH MULTITEMPORAL REMOTE SENSOR DATA Final Technical Report, 15 May 1974 - 14 Mar. 1975 (Environmental Research Inst. of Michigan) 99 p HC $4.75 CSCL 08B G3/43
N75-27534
Unclas
28784

NASA CR-141896
ERIM 109600-19-F

Final Report

STUDIES OF RECOGNITION WITH MULTITEMPORAL REMOTE SENSOR DATA

WILLIAM A. MALILA, ROSS H. HIEBER
AND RICHARD C. CICONE
Infrared and Optics Division

MAY 1975

Prepared for

NATIONAL AERONAUTICS AND SPACE ADMINISTRATION

Johnson Space Center
Earth Observations Division
Houston, Texas 77058
Contract No. NAS9-14123, Task VI
Technical Monitor: Dr. A. Potter/TF3

ENVIRONMENTAL
RESEARCH INSTITUTE OF MICHIGAN
FORMERLY WILLOW RUN LABORATORIES. THE UNIVERSITY OF MICHIGAN
BOX 618•ANN ARBOR•MICHIGAN 48107

TECHNICAL REPORT STANDARD TITLE PAGE

1. Report No.	2. Government Accession No.	3. Recipient's Catalog No.
NASA CR-ERIM 109600-19-F		

4. Title and Subtitle	5. Report Date
STUDIES OF RECOGNITION WITH MULTITEMPORAL REMOTE SENSORED DATA	May 1975
	6. Performing Organization Code

7. Author(s)	8. Performing Organization Report No.
William A. Malila, Ross H. Hieber, and Richard C. Cicone	109600-19-F

9. Performing Organization Name and Address	10. Work Unit No.
Environmental Research Institute of Michigan Infrared and Optics Division P. O. Box 618 Ann Arbor, Michigan 48107	Task VI
	11. Contract or Grant No. NAS9-14123
	13. Type of Report and Period Covered Final Technical Report May 15, 1974 to March 14, 1975
12. Sponsoring Agency Name and Address National Aeronautics and Space Administration Johnson Space Center Houston, Texas 77058	14. Sponsoring Agency Code

15. Supplementary Notes

The work was performed for the Earth Observations Division.
Dr. Andrew Potter (TF3) was contract monitor.

16. Abstract

Characteristics of multitemporal data and their use in recognition processing was investigated. Principal emphasis was on satellite data collected by the LANDSAT multispectral scanner (MSS) and on temporal changes throughout a growing season. The motivation for the studies was LACIE . Since multitemporal LACIE data were not available for the study, CITARS data were used instead, with corn and soybeans as the major crops and a small amount of winter wheat.

Three studies are reported. The first is of the effects of spatial misregistration on recognition performance with multitemporal data. A new capability to compute probabilities of detection and false alarm was developed and used with simulated distributions for misregistered pixels . A two-time-period case was simulated in this initial study. Wheat detection was found to be degraded and false alarms increased by misregistration effects. Recommendations are made for continued analysis of this problem in LACIE applications .

The second study was of multitemporal signature characteristics and multitemporal recognition processing and was made to gain insights into problems associated with this approach and possible improvements. Empirical and simulation studies of signatures showed substantial variability within some cover classes. Recognition performance with one multitemporal data set did show marked improvements over results from single-time data, especially for crop proportion estimates for full sections of test data. Further investigations on LACIE data sets are recommended. Also recommended are measurements of wheat reflectance characteristics. (See next page)

17. Key Words	18. Distribution Statement
Multitemporal Recognition, Multispectral Remote Sensing, LANDSAT, Spatial Registration, Interpretive Techniques, Thermal	Initial distribution is indicated at the end of this document

19. Security Classif. (of this report)	20. Security Classif. (of this page)	21. No. of Pages	22. Price
Unclassified	Unclassified	99	

16. Abstract (Continued)

Thirdly, time of day effects on multispectral recognition performance were studied in aircraft MSS data. Degradations associated with the passage of time were found to be substantial but largely correctable by signature adjustments based on average signals over the scene. Corrections based only on theoretical sun-angle corrections were inferior. Incidental to the reported study, calculations showed that the thermal channel was preferred for single-time recognition.

PREFACE

This document reports processing and analysis efforts on one task of a comprehensive and continuing program of research in multispectral remote sensing of the environment. The research is being carried out for NASA's Lyndon B. Johnson Space Center, Houston, Texas, by the Environmental Research Institute of Michigan (ERIM). The basic objective of this program is to develop remote sensing as a practical tool for obtaining extensive environmental information quickly and economically.

The specific focus of the work reported herein was the application of multitemporal remote sensing techniques to agricultural inventory problems. The first two of three studies dealt with multispectral scanner (MSS) data from the LANDSAT-1 satellite, while the third considered aircraft MSS data.

The research covered in this report was performed under Contract NAS9-14123 during the period 15 May 1974 to 14 March 1975. Dr. Andrew Potter (TF3) served as the NASA Contract Technical Monitor. At ERIM, work was performed within the Infrared and Optics Division, headed by Richard R. Legault, Vice-President of ERIM, in the Information Systems and Analysis Department, headed by Dr. Jon D. Erickson. Mr Richard F. Nalepka, Head of the Multispectral Analysis Section served as Principal Investigator.

The authors wish to acknowledge the assistance of other members of the ERIM staff in addition to those cited above. Jane E. Sarno assisted in portions of the processing effort. W. Richardson, D. Rice, H. Horwitz, and R. Crane were consulted in the formulation of the model for misregistered-

pixel distributions and/or in the development of a computer program to compute probabilities of misclassification for fixed decision boundaries. The ERIM number of this report is 109600-19-F.

CONTENTS

FIGURES

TABLES

1

SUMMARY, CONCLUSIONS, AND RECOMMENDATIONS

The characteristics of multitemporal data and their use in recognition processing were investigated for an agricultural application. Principal emphasis was on satellite data collected by the LANDSAT-1 multispectral scanner (MSS) and on temporal changes that occur throughout a growing season. Also, a previously reported study of temporal changes throughout the course of one day in aircraft MSS data was completed.

The objectives of the investigations were directed toward the Large Area Crop Inventory Experiment (LACIE)*, but the only multitemporal data available for analysis during the course of this investigation were from the CITARS (Crop Identification and Technology Assessment for Remote Sensing)** task. The primary crops in the data were corn and soybeans, with a small amount of winter wheat in June of the 1973 growing season.

One objective was to begin a study of the effects of spatial misregistration errors on computer recognition performance with multitemporal data. A substantial amount of progress was made in setting up the problem and, through simulation, getting initial indications of the potential severity of misclassifications attributable to spatial misregistration in a two-time-period situation. A capability was developed to compute probabilities of

---

*LACIE is a multi-agency (NASA, NOAA, USDA) project which is developing a capability for using multitemporal LANDSAT data to inventory wheat acreage and estimate its production.

**CITARS is a NASA/USDA project which preceded LACIE and focussed primarily on corn and soybean acreage estimation. Recognition processing was performed by three organizations (NASA Johnson Space Center, Purdue/LARS, and ERIM) and results are being compared using analysis of variance techniques.

classification for any signature distribution with respect to the optimum linear decision surface defined by any given pair of signatures. This capability was employed along with previously developed techniques to compute probabilities of detection and false alarm for a variety of distributions for misregistered pixels. The results indicate that the inclusion of some other ground covers in second-time-period wheat pixels, through misregistration, could degrade recognition performance substantially. Furthermore, it was shown that false alarms from misregistered pixels of other ground covers could be greater than from pure samples of these other crops. Recommendations are made for continued and expanded analysis of this problem in LACIE applications; these are detailed in Sec. 3.7.

A second objective was to study multitemporal signatures and recognition processing with multitemporal data to gain insights into problems associated with this approach and possible improvements. Empirical studies of signatures from LANDSAT-1 MSS data were made, as well as some simulations with a vegetation canopy reflectance model and a radiative-transfer model. Recognition processing was performed using the ERIM linear decision rule on a multitemporal data set for the Fayette segment of CITARS. Substantial variability in ground conditions and MSS signals was found within some of the ground cover classes, especially soybeans. Indications were that training data did not adequately represent all conditions of some crops in the test areas. Nevertheless, recognition performance with the multitemporal data did show marked improvements over that with data from the best single time for recognition, especially in crop proportion estimates

for full sections of test data. Results with this one data set are encouraging and further investigations should be conducted on other sets, especially of LACIE data. It also is recommended that measurements be made of wheat leaf reflectances and transmittances and canopy structures for different wheat varieties and conditions, as well as wheat field reflectances. These data would be invaluable in simulation studies of wheat signatures because the limited measurements presently available indicate wide variability in wheat reflectance characteristics.

The third objective considered in this report was to investigate (1) the changes which occur in multispectral signatures throughout a period of several hours, (2) their effect on recognition performance, and (3) the capabilities of three signature extension preprocessing methods to correct for the effects. The data set studied was collected by an aircraft MSS scanner on a series of passes over the same ground site throughout one day. Severe degradation in recognition performance was found when unadjusted signatures from the first pass were applied to later passes . Of the three methods tested, signature adjustments based on average signals over the scene proved to be the best, while those based only on theoretical sun-angle corrections were the poorest (although they did offer some improvement over unadjusted signatures). While incidental to the reported study, we note that calculations of optimum channels for discrimination showed the thermal channel to be preferred for recognition with signatures extracted from the data pass analyzed; second preference was for near-infrared channels.

2
INTRODUCTION

Until recently, the major features exploited during recognition processing of remote sensor data have been the spectral differences sensed by multispectral scanners. Now, use of the temporal characteristics, as well, of multispectral scanner signals is under investigation and development, e.g., in the Large Area Crop Inventory Experiment (LACIE). For systems that use LANDSAT data, the basic temporal interval between passes is 18 days and collection over a span of several months is possible. This temporal sampling interval and span are such that one can use the varied phenological patterns of different ground covers in the differentiation process.

In order to carry out recognition processing with multitemporal data, it is necessary to place data from two or more dates into spatial registration. In this registration process, there will be misregistration errors whose magnitudes depend on the technique used for registration, as well as on characteristics of the data set. The objective of one of the subtasks here was to begin a study of the effects of misregistration errors on computer recognition performance with multitemporal data.

Given spatially registered data, one next requires relatively unique signatures for the crops and ground covers that are to be differentiated. By signatures, we mean the statistical parameters (e.g., mean vector and variance-covariance matrix) which are used to describe the multitemporal multispectral signals from the various ground covers. Signatures from all types of surfaces change throughout the year as the sun changes position and atmospheric conditions change. Yet, the signatures of vegetative covers

change in additional ways throughout the growing season, so it is of interest to analyze and determine how best to take advantage of these phenological changes for differentiation and recognition.

Thus, another part of our multitemporal task dealt with studies of multitemporal signatures. The CITARS (Crop Identification Technology Assessment for Remote Sensing) effort [1] provided a multitemporal set of LANDSAT-1 data on which we performed empirical studies of signature characteristics. Corn and soybeans are the major crops for which data were available for more than two 18-day cycles. Therefore, a majority of this effort was devoted to these crops. Signatures were extracted and analyzed both for specific fields in the scene and for clusters of data that were defined by a clustering algorithm which operated on the data points independent of field boundaries.

We had anticipated analyzing multitemporal signatures for wheat in LACIE data. However, the data were not received in time for analysis and inclusion in this report. Since there was a limited amount of data for wheat in the CITARS data set, these were examined.

Valuable insights into signature characteristics can be obtained through the use of simulation models. In addition to the empirical analysis of LANDSAT signatures, we performed some theoretical calculations with a reflectance model for vegetation canopies and a radiative transfer model to simulate atmospheric effects for satellite sensors.

---

[1] Malila, W. A., D. P. Rice, and R. C. Cicone, "Final Report on the CITARS Effort by the Environmental Research Institute of Michigan", Report No. NASA CR-ERIM 109600-12-F, Environmental Research Institute of Michigan, Ann Arbor, Michigan, February 1975.

An end objective of the task was to investigate methods for improving recognition performance with multitemporal data from the LANDSAT multispectral scanner. A series of recognition runs was made with various sets of signatures to explore the degree to which each set represented the data from test fields.

The final topic of this report concerns temporal variations that occur throughout the period of one day rather than the period of weeks and months with LANDSAT data. The data were collected by an airborne multispectral scanner on a series of flights over the same test site throughout one day. The changes in signals throughout the day and methods for correcting for them were examined. The effort reported herein is a continuation and conclusion of work that was begun and partially reported under last year's contract [2].

---

[2] Malila, W. A., R. H. Hieber, and J. E. Sarno, "Analysis of Multispectral Signatures and Investigation of Multi-Aspect Remote Sensing Techniques", Report NASA CR-ERIM 109100-27-T, Environmental Research Institute of Michigan, Ann Arbor, Michigan, July 1974.

3

EFFECTS OF SPATIAL MISREGISTRATION ON RECOGNITION

Misregistration of ERTS data from two or more time periods can introduce errors in multitemporal recognition results. The objective of this subtask was to begin an investigation that will assess the severity of this problem in the LACIE context.

A multitemporal data set may consist of as few as two and as many as five or more time periods of data for a given area of interest. Generally, a specific time period is chosen as the base or reference period and data from the others spatially registered to this 'base' data set. Ideally, the data values from each time period that are associated with a given multitemporal picture element (pixel) will represent the same location on the ground. However, different data collection geometries on the various passes would cause misalignment of the sampling grids; the commonly used, nearest-neighbor algorithm for interpolating data values maximizes differences due to non-overlapping sampling grids. Furthermore, inaccuracies of the registration algorithm itself may lead to additional misregistration of data pixels, so the family of associated single-time pixels would not be representing exactly the same ground area. A pixel which was entirely wheat in the base time period may be associated with one in another time period that contains a boundary and a portion of a neighboring crop, for example it may represent a mixture of 70% wheat and 30% corn.

3.1 APPROACH

The initial approach taken has been to consider two time periods, T_1 and T_2, and assume that pure field-center pixels exist for the first time period. The T_2 pixel that is associated with a T_1 pixel then may be either: (1) perfectly registered, (2) misregistered but still within the same field as the T_1 pixel, (3) misregistered and crossing the boundary between the field and another ground cover so the pixel signal vector represents a mixture of the two ground covers, or (4) totally in another field. The first case is the ideal situation and is considered to be the reference condition. All but case (2) are studied in this report.

A model was established to simulate the effects of misregistration on classification accuracy. A simulation approach was taken to determine, without having to handle large amounts of data, the extent to which classification accuracy would deteriorate given varying degrees of misregistration. It also helped to clarify the problems that would be confronted in processing real data. A two-time-period multitemporal situation was chosen for initial study to avoid complications associated with more time periods. Wheat was the major crop of interest, and data supplied through the CITARS task were used as a basis for the simulation.

Signatures were simulated for crops with a variety of misregistrations. Probabilities of correct classification then were computed and analyzed for two types of decision boundaries: (1) the shifting (i.e., pairwise) linear decision boundary* between the wheat distribution and each simulated

---

*The linear decision boundaries used for this report were determined by the ERIM 'best linear' decision rule [3] which minimizes average pairwise probability of misclassification and has been shown to provide recognition performance comparable to quadratic decision rules at a lower cost.

[3] Crane, R. B., and W. Richardson, "Performance Evaluation of Multispectral Scanner Classification Methods", Proceedings of the Eighth International Symposium on Remote Sensing of Environment, Vol. II, Report No. 195600-1-X, Environmental Research Institute of Michigan, Ann Arbor, Michigan, 1972, pp. 815-31.

misregistered distribution and (2) the fixed linear decision boundaries between wheat and the other pure crop distributions. It was found in both analyses, though more dramatically in the second analysis, that even small amounts of misregistration would introduce significant errors in the classification of pixels at or near boundaries between fields.

3.2 DESCRIPTION OF MODEL

A multispectral signature for material W consists of a mean vector A_W and a variance-covariance matrix C_W. We introduce the following notation to simplify the discussion of multitemporal (two-time-period) signatures and the simulation of misregistration effects. Let (A_{W1}, A_{W2}) denote the mean vector A_W, where the component vectors A_{W1} and A_{W2} represent the multispectral signal means in time periods one and two, respectively. Further, partition the variance-covariance matrix as follows:

$$C_W = \left(\begin{array}{c|c} C_{W1,W1} & C_{W1,W2} \\ \hline C_{W1,W2} & C_{W2,W2} \end{array}\right) \qquad (1)$$

where the four partitions are equal-sized matrices. $C_{W1,W1}$ represents the covariance of crop W in time period one and $C_{W2,W2}$ that in time period two. $C_{W1,W2}$ then represents the covariances between signals from the two time periods for individual pixels. The diagonal partitions can be empirically determined separately from data sets at the two time periods. However, the off-diagonal partitions can be determined empirically only from spatially registered multitemporal data under limitations imposed by the registration accuracy.

Now, consider the case where, because of misregistration, the pixels during the second time period represent mixtures of ground cover W and some other ground cover O. The question arises as to what model should be used to construct the signature of misregistered pixels from the pure signatures of W and O.

The misregistered mean vector A_M simply consists of the mean vector of cover W for time period one and the weighted sum of the two constituent mean vectors for time period two:

$$A_M = A_{W1,}\ [\alpha A_{W2} + (1-\alpha)\ A_{02}] \tag{2}$$

where α is the proportion of cover W present in each pixel for time period two and $(1-\alpha)$ is the corresponding proportion of cover O.

The definition of the variance-covariance matrix is not quite as straightforward. Obviously, one would retain $C_{W1,W1}$ as the first of the four partitions of the matrix. For time period two, we chose to use the ERIM mixtures-model representation [4] of the covariance of mixture pixels, namely:

$$C_{M2,M2} = \alpha C_{W2} + (1-\alpha)\ C_{02} \tag{3}$$

where the subscript M2 denotes the misregistered mixture pixels in time period two. It is not immediately evident how one should determine coefficients of the two off-diagonal matrices $C_{W1,M2}$. For the work reported here, we have assumed them to be zero:

$$C_{W1,M2} = 0 \tag{4}$$

---

[4] Nalepka, R. F., H. M. Horwitz, and P. D. Hyde, "Estimating Proportions of Objects from Multispectral Data", Report NASA CR-WRL 31650-73-T, Willow Run Laboratories, University of Michigan, Ann Arbor, Michigan, March 1972.

which represents a complete lack of correlation between the signals from the pure W pixels in time period one and the mixture pixels of time period two.

3.3 DESCRIPTION OF ANALYSES UNDERTAKEN

Given a representation of the signal distributions of misregistered pixels, as above, we next considered ways of estimating the effects of misregistration on recognition performance. A computer program was written to generate signatures for misregistered pixels with varying degrees of misregistration (parameter $1-\alpha$ in Eqs. 2-4). Given these representations, two techniques were used in the analysis .

First, a linear decision boundary was determined between each pair of pure crop distributions and simulated misregistered distributions. Based on this boundary for any pair of signatures, the probabilities of classifying a pixel from each signature distribution as one or the other distribution was calculated using an existing IBM 7094 computer program DISST.* Note that, since the decision boundary was dependent on the simulated signature, the boundary would shift for different values of α. This would not totally describe the real situation in which the decision boundaries between pure crop signatures would remain fixed and misregistered pixels would be classified with respect to these boundaries regardless of degree (measured by parameter $1-\alpha$) of misregistration. To correct for this deficiency, a second technique was developed. A new program POC was written to calculate the probability of classifying any given third

*The calculation of the probabilities assumes multivariate normal distributions, uses procedures developed by the authors of Ref. 3, and was implemented by D. Rice; all are with ERIM.

distribution as one or the other of a given pair of distributions, based on the fixed boundary between the given pair.*

3.3.1 ANALYSES UNDERTAKEN WITH PROGRAM DISST

DISST computes several quantities for pairs of multispectral signatures: (a) the χ^2 distance of the mean of one distribution from the mean of the other, measured in terms of the covariance matrix of the latter, (b) the average probability of misclassification between the two distributions according to the best linear decision rule, and (c) the separate probabilities of misclassification which are averaged to obtain (b). Values of these quantities for a variety of misregistration conditions were calculated. These values were used as an indication of the effects of varying degrees of misregistration on recognition performance.

The χ^2 distance was a measure of how far a misregistered distribution moved away from the pure distribution of the crop as varying degrees of misregistration were introduced. The probabilities of misclassification quantified to some extent the degree of decay that would be experienced in recognition performance as the degree of misregistration increased. The highest possible calculated value is 50%, the probability of classifying, for example, wheat as wheat. As illustrated in Fig. 1 for a one-dimensional case, the shaded area to the left of the decision line represents the probability that distribution M will be classified as distribution W. As the means of the two distributions approach each other, this

*This second calculational technique is an adaptation of the first and was implemented by R. Cicone after consultation with those noted in the preceding footnote.

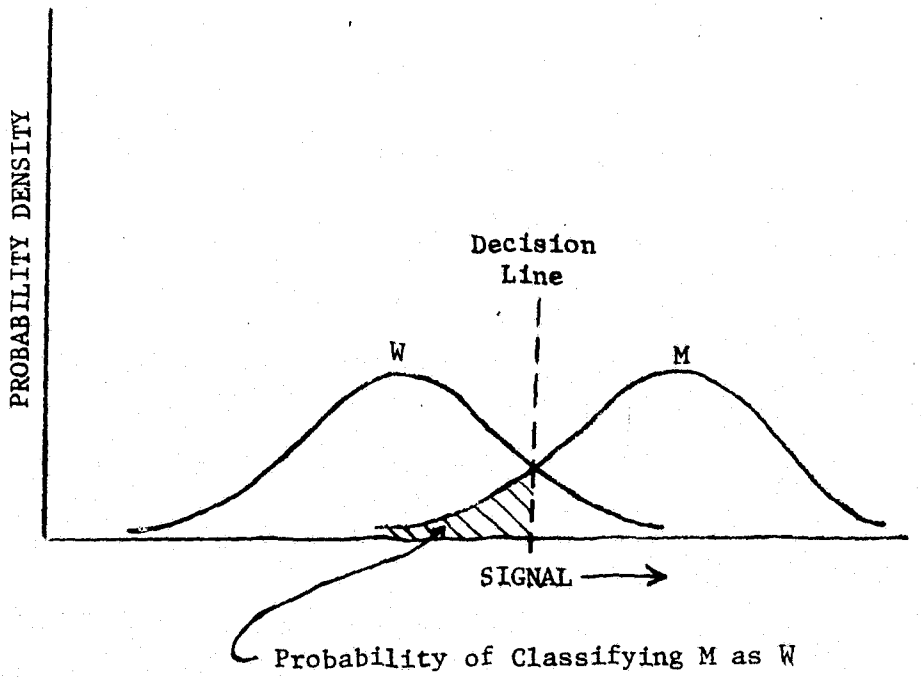

FIGURE 1. ILLUSTRATION OF PROBABILITY OF CLASSIFICATION

probability of classification increases. Finally, if the means were to coincide, half of the distribution still would lie to the left of the decision line which also would coincide with the means.

3.3.2 ANALYSES UNDERTAKEN WITH PROGRAM POC

Given three distributions W, O, and X, program POC calculates the probability of classifying distribution X as either W or O based on the linear decision boundary between W and O. The highest possible calculated value is 100%, i.e., that pixels from distribution X will always be classified as one of the two other distributions. The calculation of the probability of classification by POC, with respect to a decision boundary that is independent of the distribution in question, affords one a distinct advantage over the probabilities of misclassification determined by DISST. Probabilities of incorrectly classifying spatially misregistered multitemporal pixels were determined for varying degrees of misregistration (measured by parameter $1-\alpha$) with respect to a fixed boundary. Then a recognition curve was graphed, based on calculations for various α's, so that changes in the rate of recognition decay could be visualized as misregistration became more significant. As will be discussed later, it was discovered that for some combinations of misregistration even small values of $(1-\alpha)$ will cause rapid deterioration of recognition performance.

3.4 DESCRIPTION OF DATA SET STUDIED

Having presented a description of the problem faced, the simulation model chosen, and the two analytical tools at our disposal, let us now turn our attention to the data set chosen as the basis for our initial

analysis of the effects that misregistration of multitemporal data may have on recognition accuracy.

Wheat was chosen the crop of primary interest, because of the LACIE interest in this crop. The simulation was based on empirical signatures of multitemporal CITARS data from the Fayette segment on 10 June and 29 June 1973 [1].

Eight-channel signatures were extracted for individual fields from the spatially registered CITARS data set. The pixels from the various time periods had been associated using a nearest neighbor rule. The assumption was made that the two data sets were perfectly registered. The individual field signatures for wheat, water, trees, corn, and soybeans were then combined to form five class signatures. Table 1 presents means and standard deviations for these signatures -- the first four channels represent the ERTS bands for 10 June and the last four for 29 June. Fig. 2 presents spectral plots of the data in Table 1.

In the combination process, a few outlier fields were rejected from the final signatures (χ^2 rejection thresholds of 8.0 and 20.1 were used in a two-pass procedure). One field was rejected out of eleven fields of wheat; none of three water fields, three of forty corn fields, four of fifty-nine soybean fields, and one of thirteen tree 'fields' were rejected.

Fig. 2, presenting the spectral plots of the 'pure' crop signatures, indicates some interesting patterns that are useful to discuss presently for purposes of the analysis to come.

---

[1] Malila, W. A., D. P. Rice, and R. C. Cicone, "Final Report on the CITARS Effort by the Environmental Research Institute of Michigan", Report No. NASA CR-ERIM 109600-12-F, Environmental Research Institute of Michigan, Ann Arbor, Michigan, February 1975.

TABLE 1. MEANS AND STANDARD DEVIATIONS OF MULTITEMPORAL SIGNATURES FOR FAYETTE 10 AND 29 JUNE 73

	10 June				29 June				
	Ch. 1 Band 4*	Ch. 2 Band 5	Ch. 3 Band 6	Ch. 4 Band 7	Ch. 5 Band 4	Ch. 6 Band 5	Ch. 7 Band 6	Ch. 8 Band 7	
Water	37.39	30.95	20.27	4.87	40.05	38.58	27.75	7.28	means
	1.48	2.00	3.22	2.65	2.02	2.22	4.76	2.10	std. dev.
Tree	29.36	18.46	60.31	35.79	24.36	14.94	56.64	35.77	
	2.40	3.47	3.43	2.85	2.33	2.97	4.85	2.51	
Corn	45.21	46.68	50.10	23.56	31.28	26.03	26.93	25.93	
	6.27	9.07	8.67	3.95	2.91	4.39	6.87	4.50	
Soybean	46.71	48.12	51.86	24.73	36.47	36.18	43.66	21.95	
	7.54	11.62	9.27	4.39	3.82	6.46	6.17	3.10	
Wheat	36.70	30.39	51.60	27.20	33.18	29.65	51.40	28.45	
	5.92	9.84	9.63	6.61	3.08	6.30	8.52	6.51	

Final CITARS Wheat Signatures

	10 June				29 June			
	Band 4	Band 5	Band 6	Band 7	Band 4	Band 5	Band 6	Band 7
Wheat	33.93	27.48	43.33	22.03	34.66	34.29	49.14	26.12
	1.30	2.17	4.03	3.13	2.85	5.80	7.93	5.88

*LANDSAT-1 Bands

FIGURE 2. MULTITEMPORAL SIGNATURE SPECTRAL CURVES

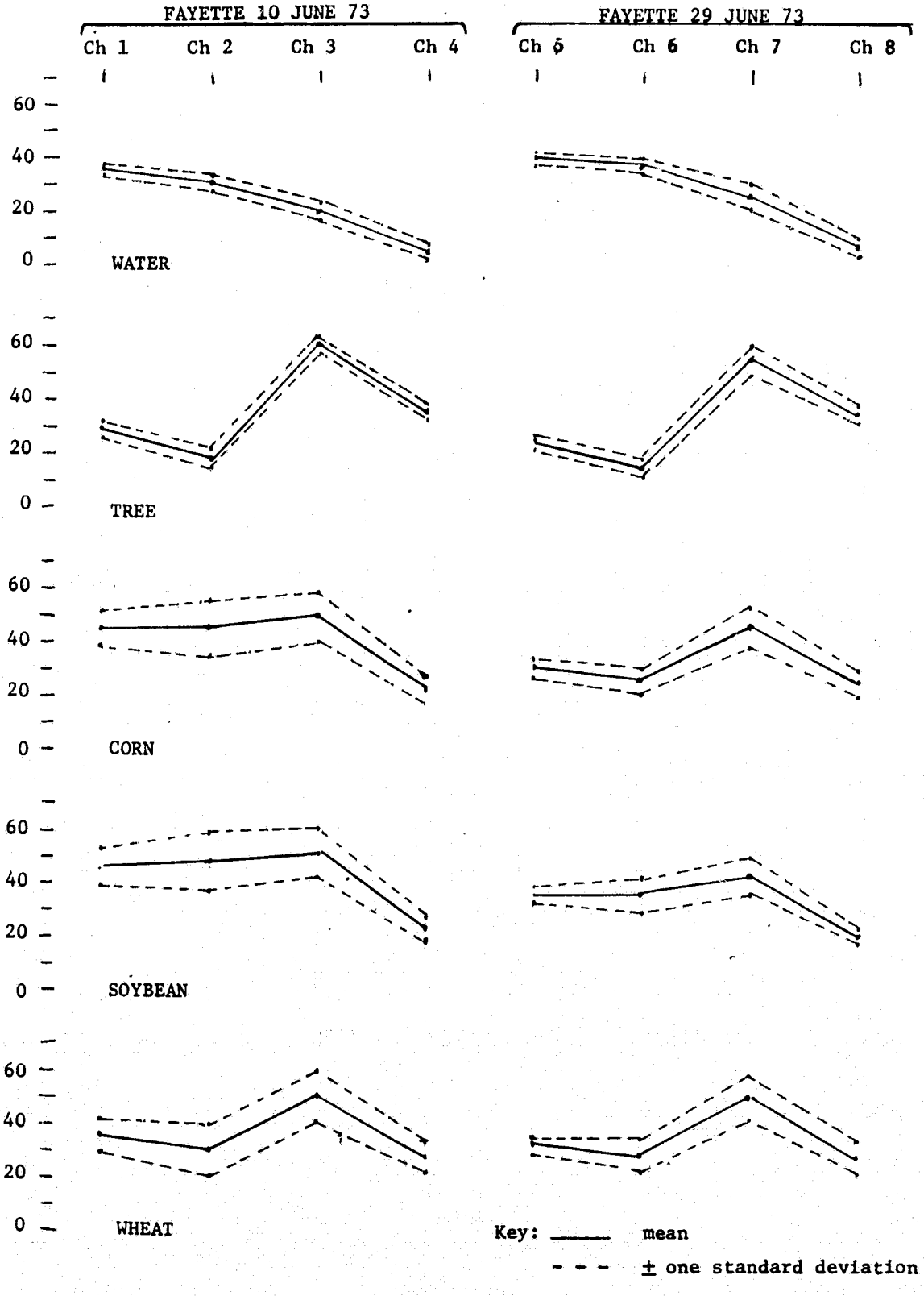

The spectral shapes of water, tree, and wheat signatures remain relatively constant from time period one to two. From Table 1 we find that the water signature signal values shifted up in going from the first to the second time period while those for trees shifted down. Wheat values remained relatively constant from one time period to the next. Corn and soybeans looked alike in early June, when both were primarily bare soil, but were different in late June. Soybean cover increased slowly so the soybean signature in late June bears a strong resemblance to the early-June signature. Corn on the other hand had a late-June spectrum that indicates a substantial amount of green vegetation mixed with soil. Note also the similarity between corn and wheat spectra in the late-June period, though corn had somewhat higher values than wheat.

A computer program was written to generate signatures for misregistered pixels with varying degrees of misregistration (parameter $1-\alpha$ in Eq. 2-4). The program was used to simulate misregistrations during the second time period of 1/3, 2/3, and a complete pixel (or more) for all pairs of the five ground covers. A total of 60 misregistered-pixel signatures were generated.

There are some reservations with respect to the 'pure' wheat signature that should be mentioned. Due to the scarcity of wheat training fields available, a number of test wheat fields were also used in determining the signature of wheat for the analyses presented here. These included at least one large field whose ground truth designation has been since brought into question [1]. A comparison with the final wheat signatures determined and

---

[1] Malila, W. A., D. P. Rice, and R. C. Cicone, "Final Report on the CITARS Effort by the Environmental Research Institute of Michigan", Report No. NASA CR-ERIM 109600-12-F, Environmental Research Institute of Michigan, Ann Arbor, Michigan, February 1975.

used in CITARS for 10 June Fayette showed the multitemporal signature to be higher in value in time one with more than twice the standard deviation (See Table 1). It would be of interest to repeat the analysis using the CITARS signatures. It also would be appropriate to suggest that other data sets, preferably LACIE data, could be prepared and analyzed in a similar fashion for confirmation and extension of the results presented herein. No such data were available in time for analysis and inclusion in this report.

3.5 ANALYSIS OF VALUES CALCULATED BY DISST

Let us now turn our attention to the analysis of various values calculated for the stated data set and simulation model. Recall from Sec. 3.3.1 that calculations by program DISST include: (1) χ^2 distance, (2) average pairwise probabilities of misclassification, and (3) separate probabilities of misclassification.

3.5.1 ANALYSIS OF THE PROBABILITIES OF DETECTION

Fig. 3(a) displays the relative probabilities that a misregistered wheat pixel would be recognized as wheat for four mixture crops. At one extreme, a misregistration of only 1/3 a pixel of water into the second time period of wheat reduced the relative probability of classifying the pixel as wheat from 1.0 to 0.5; this is reduced to 0.06 for 2/3 a pixel of water and essentially zero for a full pixel of water at time period two. At the other extreme, there was no reduction for 1/3 corn at time two and reductions only to 0.92 for 2/3 corn and 0.66 for all corn at time two. Results for soybeans and trees were intermediate.

FIGURE 3. QUANTITIES CALCULATED WITH PROGRAM DISST.

FIGURE 3(a) PROBABILITY OF CLASSIFYING A MISREGISTERED MULTITEMPORAL WHEAT PIXEL AS WHEAT, BASED ON THE BEST LINEAR DECISION BOUNDARY BETWEEN THE WHEAT DISTRIBUTION AND THE SIMULATED MISREGISTERED WHEAT DISTRIBUTION.

FIGURE 3(b) χ^2 DISTANCES OF MISREGISTERED PIXELS FROM WHEAT IN TERMS OF THE WHEAT COVARIANCE MATRIX.

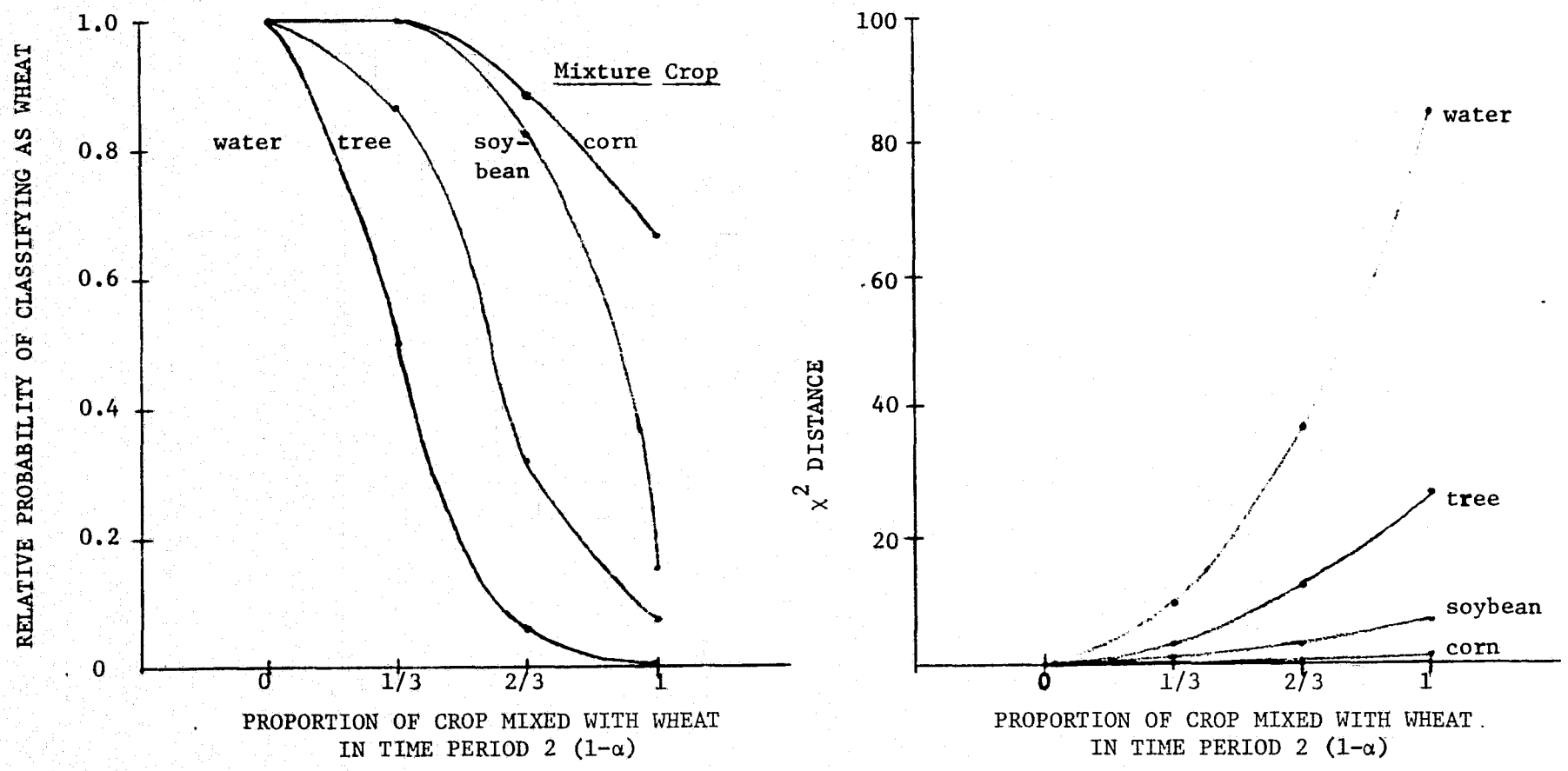

Keep in mind that the values computed and displayed in Fig. 3(a) are not exactly representative of the effects of misregistration on recognition performance. The reason is that the decision line between the pure and misregistered wheat distributions moves as the amount of misregistration changes, rather than remaining fixed as it would for a given set of signatures used in recognition. One can, however, begin to get a feeling here of the relationship between pure wheat and misregistered wheat distributions, and the same general trends are found with fixed boundaries (Sec. 3.6), although specifics differ. Quite obviously as the misregistration parameter $(1-\alpha)$ increases in value, the misregistered wheat pixel moves away from the wheat distribution at a rate dependent on the mixture crop. The rate of that movement cannot be measured exactly by those values displayed in Fig. 3(a) since the boundary line is dependent on the covariance of the misregistered pixels.

3.5.2 ANALYSIS OF THE χ^2 DISTANCES CALCULATED BY DISST

A measure that is independent of the covariance of misregistered pixels is the χ^2 distance of their mean value from the mean of the wheat distribution, the χ^2 measure being based on the covariance matrix of the wheat distribution. Fig. 3(b) presents χ^2 distances corresponding to the probabilities plotted in the previous figure. Whereas the probabilities of classification as wheat decreased monotonically as the amount of misregistration increased, the χ^2 distances correspondingly increased.

It is of interest at this point to discuss these calculated results with respect to the multitemporal signature spectral curves (Fig. 2). Note that misregistration of corn into time-two wheat pixels causes the mean of the misregistered pixel to remain very near the mean of the wheat distribution.

This is not surprising since, as previously mentioned, the spectral curves of corn and wheat in time period two are very similar. On the other hand, misregistration of water into wheat forces the greatest departure from pure wheat since, of the four possible mixture crops, the spectral curve of water is least like wheat.

3.5.3 ANALYSIS OF THE PROBABILITIES OF FALSE ALARM

There also is the possibility that another ground cover might "look" more like wheat when mixed with some other cover at time period two due to misregistration. Results are portrayed in Fig. 4 for mixtures of the four other ground covers. We see that soybeans and trees both give rise to higher probabilities of misclassification as wheat when mixed with other covers at time two. Corn tends to look less like wheat when mixed and water remains very much unlike wheat. The shape of the soybean-tree (and tree-corn) curve is interesting in that a small misregistration (1/3 pixel) gives rise to a larger probability of misclassification as wheat than does a larger misregistration. In a sense this particular misregistration is pulling the soybean pixel towards wheat for small degrees of misregistration (parameter $1-\alpha$) then away from wheat as the parameter increases in value. To understand why, let us compare the time-period-two wheat, tree, and soybean spectral curves (Fig. 1). Note that the curve for wheat displays more pronounced bends at channel 6 and channel 7 than that for soybean. However, the tree curve exagerates these bends even more. The effect of adding a small amount of the tree signal values to soybean would be to make the spectral curve look very much like the wheat curve. However, if the effect of the tree curve were to become dominant, the spectral curve of the misregistered pixel would become less like wheat.

FIGURE 4. PROBABILITY OF MISCLASSIFYING A MISREGISTERED NON-WHEAT MULTITEMPORAL CROP AS WHEAT, BASED ON THE BEST LINEAR DECISION BOUNDARY BETWEEN THE WHEAT DISTRIBUTION AND THE SIMULATED MISREGISTERED CROP DISTRIBUTIONS

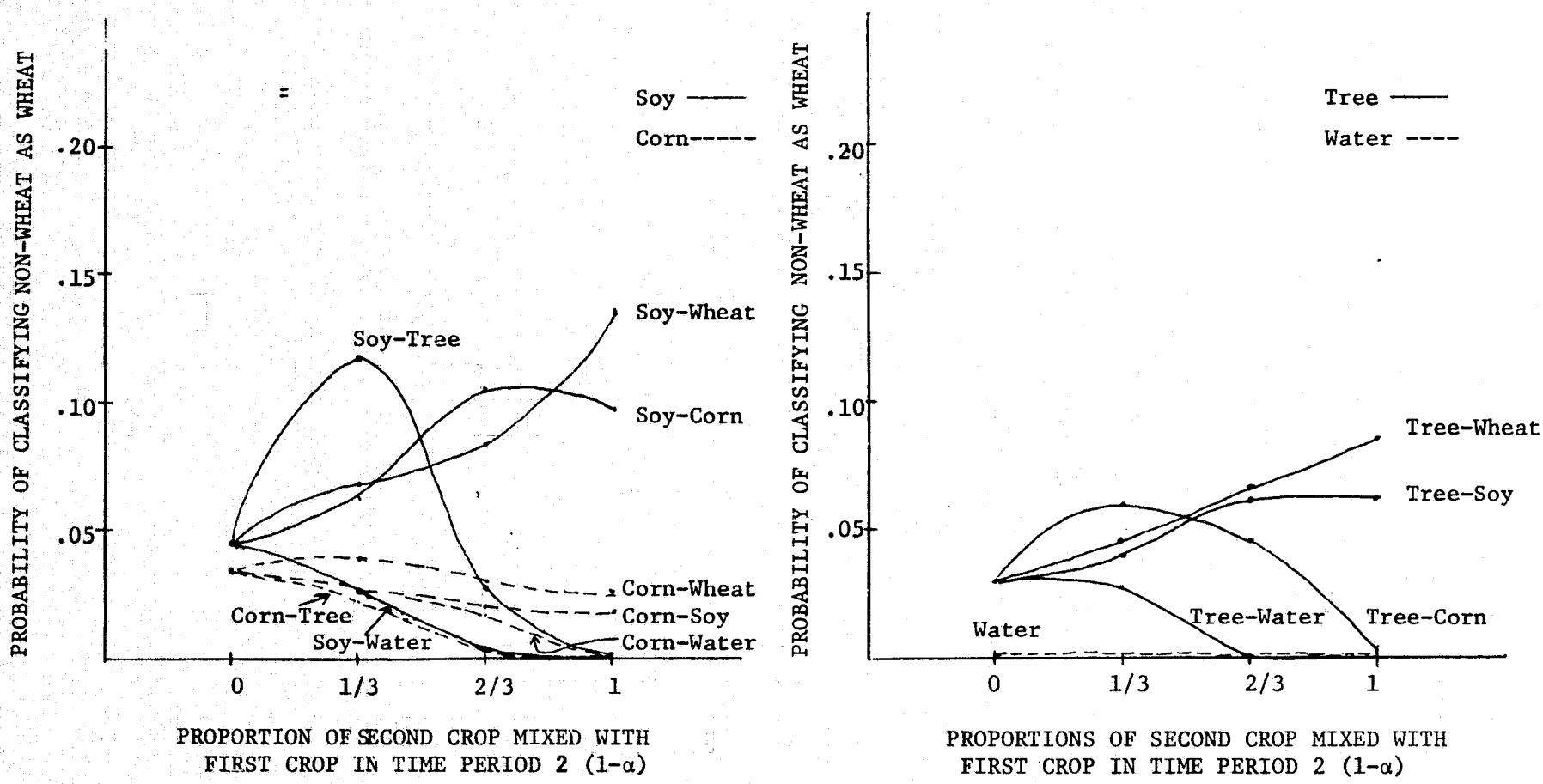

Note that the spectral curve of corn in time period two was initially very much like wheat. Misregistration of soybean or water into corn pixels results in curves sloping downward, since the only spectral effect would be to make them appear less like wheat. Whereas the curve for wheat misregistered into corn pixels remains relatively flat; whatever change does occur can be attributed to the fact that the curves in Fig. 4 are dependent on the estimated misregistered pixels covariance.

3.6 ANALYSIS OF VALUES CALCULATED BY POC

In this section, values for classification probabilities are examined that are dependent solely on the fixed boundaries between the 'pure' crop signatures. These values more accurately represent the effects of misregistration on recognition performance since it is with respect to the fixed boundaries that the classification of a misregistered pixel will be determined. We will find in this analysis an even more dramatic effect than was seen in Sec. 3.5, especially in the rate of false alarms (non-wheat called wheat).

3.6.1 ANALYSIS OF THE PROBABILITIES OF DETECTION

Fig. 5(a) displays the probability that a misregistered wheat pixel would be recognized as wheat, based on the decision boundary between wheat and the pure mixture crop. No other competing signature was introduced. Misregistration effects became most noticeably pronounced when trees were misregistered into wheat pixels. For example, 2/3 pixel of trees in time two reduced the probability of classifying the pixels as wheat to below 0.4. At the other extreme, due to the spectral similarities found between wheat and corn, the

FIGURE 5. PROBABILITY OF CLASSIFYING A MISREGISTERED MULTITEMPORAL WHEAT PIXEL AS WHEAT, BASED ON THE FIXED LINEAR DECISION BOUNDARIES BETWEEN THE PURE WHEAT DISTRIBUTION AND:

(a) THE PURE DISTRIBUTION OF THE CROP MIXED WITH WHEAT IN TIME TWO.

(b) THE PURE DISTRIBUTION OF THE CROP OTHER THAN WHEAT THAT THE MISREGISTERED PIXEL IS MOST LIKELY TO BE CLASSIFIED AS.

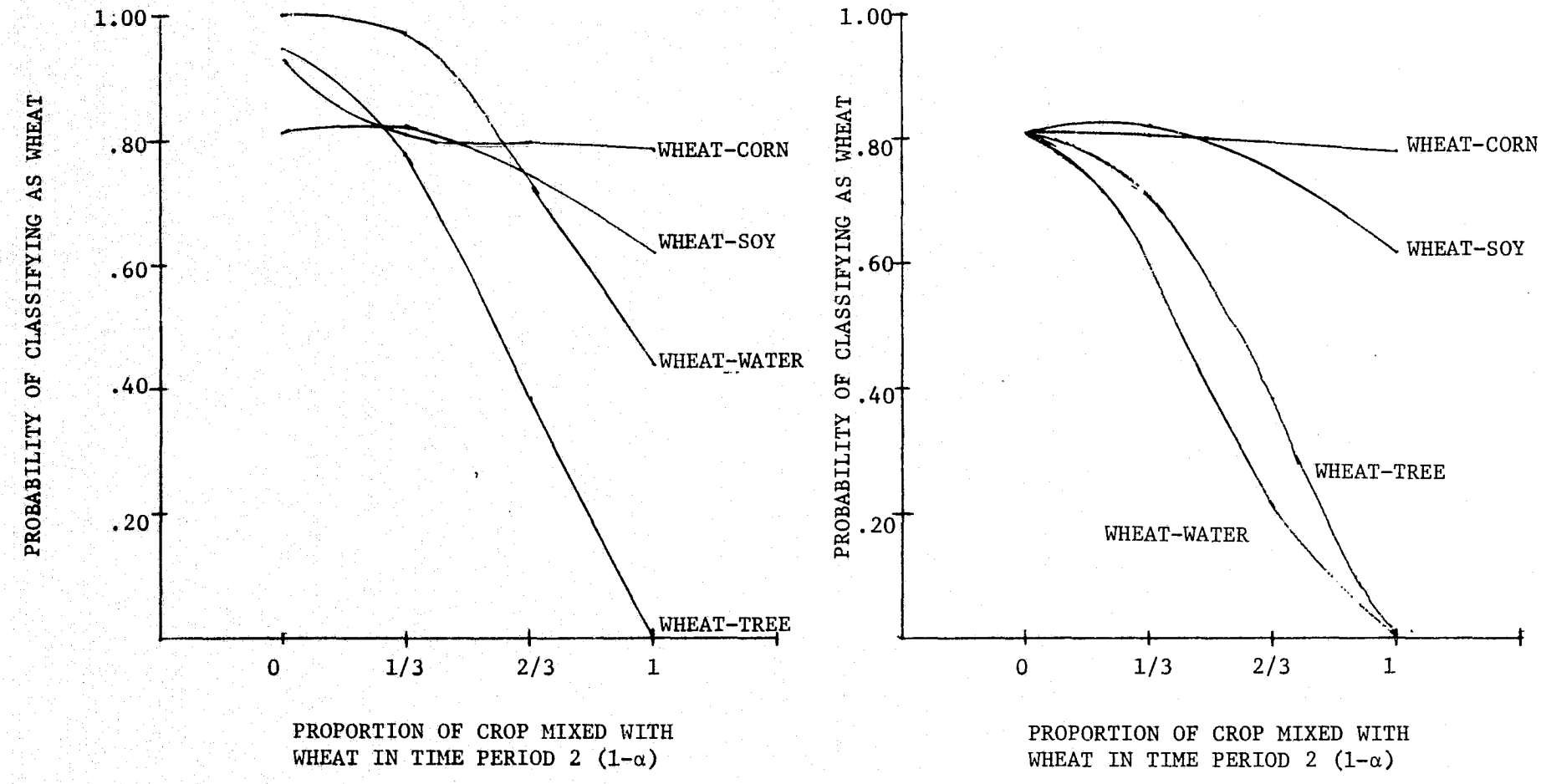

misregistration of corn into wheat pixels had relatively little effect on the probability of classifying the pixels as wheat.

It is interesting to note the recognition curves for wheat-water pixels in Fig. 5(a) versus those in Fig. 2. In Fig. 2, as previously mentioned, the wheat-water curve deteriorates most rapidly, whereas in Fig. 5(a) wheat-water values drop to a minimum of between 0.4 and 0.5. In the extreme case of misregistration, wheat pixels would be totally misregistered into water in time two. The spectral curve would then have the appearance of wheat in time period one and the appearance of water in time period two. According to calculations, maximally misregistered pixels are about as likely to be called water as they are to be called wheat, based on the wheat-vs-water decision boundaries.

Fig. 5(b) displays the minimum probability that a misregistered wheat pixel would be recognized as wheat, based on the decision boundaries between wheat and all other crops. Once again wheat-water recognition deteriorates most rapidly. The reason is that there are competing signature boundaries considered. In particular the calculations show that, given the boundary between soybean and wheat, wheat pixels with water misregistered into them at time two would tend to be called soybean, with a probability of 99% for the total misregistration case.

3.6.2 ANALYSIS OF THE PROBABILITIES OF FALSE ALARM

Fig. 6 displays the probabilities, calculated for the fixed decision boundaries, that misregistered non-wheat pixels would be recognized as wheat. The pairwise-decision-boundary counterpart of this figure is Fig. 4. The differences between corresponding curves on these two figures are much

FIGURE 6. PROBABILITY OF MISCLASSIFYING A MISREGISTERED NON-WHEAT MULTITEMPORAL CROP AS WHEAT, BASED ON THE FIXED BEST LINEAR DECISION BOUNDARY BETWEEN WHEAT AND THE DISTRIBUTION OTHER THAN WHEAT THAT THE PIXEL IS MOST LIKELY TO BE CLASSIFIED AS

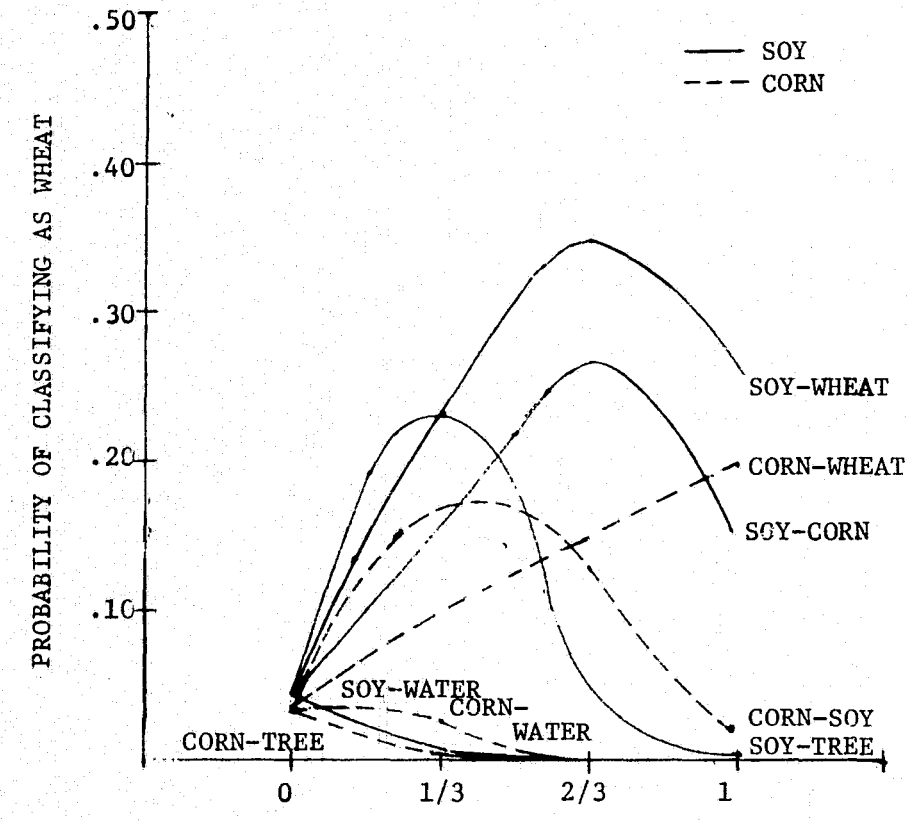

PROPORTION OF SECOND CROP MIXED WITH FIRST CROP IN TIME PERIOD 2 (1-α)

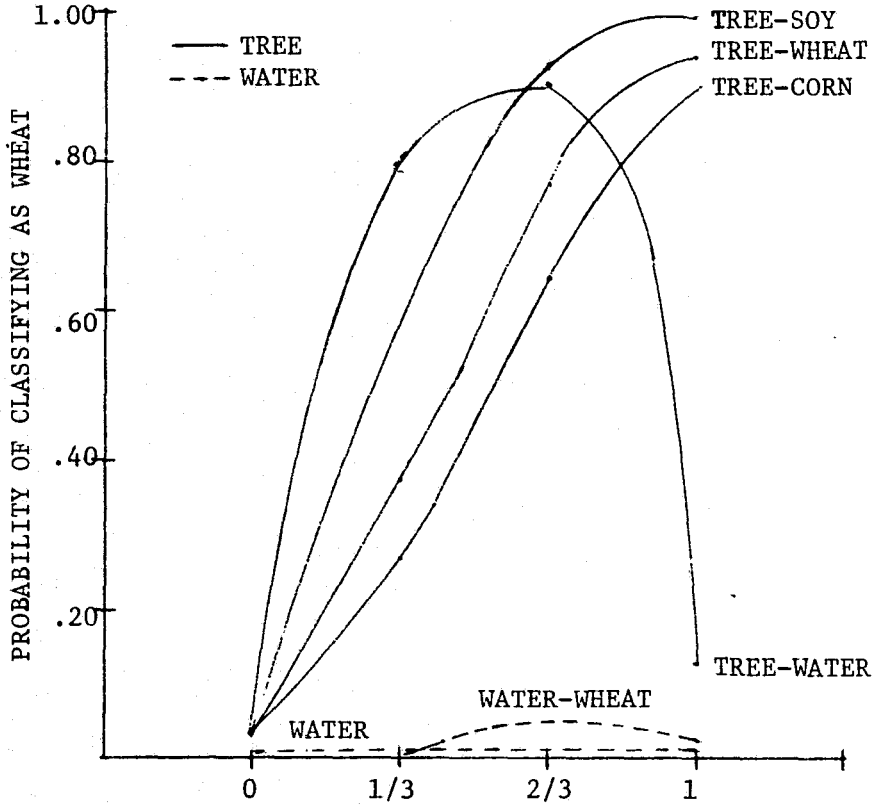

PROPORTION OF SECOND CROP MIXED WITH FIRST CROP IN TIME PERIOD 2 (1-α)

greater than the differences found in the previous subsection for wheat detection probabilities. In all cases misregistration effects on non-wheat pixel classification as wheat are much more pronounced for the fixed decision boundaries. For example, a misregistration of 1/3 water into a tree pixel in time two causes a near 0.80 probability of classifying the pixel as wheat. Total misregistration of soybean, wheat, or corn into the time-two portion of tree pixels causes the probability of misrecognition as wheat to climb as high as 0.99, 0.94 and 0.89, respectively. There also are several occurrences of an initial increase and then a decrease in wheat false-alarm probability as misregistration increases. This situation was earlier noted and explained (Sec. 3.5.3). Similar explanations can be determined here as well through examination of the given spectral curves of the various crops.

One can easily conclude after examination of these values that misregistration of non-wheat pixels can cause a sharp deterioration of the proper classification of the misregistered pixels and increase the false alarm rate for wheat.

3.7 SUMMARY, CONCLUSIONS, AND RECOMMENDATIONS

An investigation of the effects of spatial misregistration on multitemporal recognition was undertaken to quantify the extent of deterioration of recognition accuracy of given misregistered pixels. A simple model was defined and used with empirical signatures from one CITARS data set to make simulations of distributions of misregistered pixels. These simulated distributions were used to calculate both (1) probabilities of misclassification based on the best linear decision boundary between a major crop signature

and each simulated signature and (2) probabilities of classification based on fixed decision boundaries between the various class signatures, as would be encountered in recognition. The analysis concentrated on wheat as the major crop.

The results show that mixtures of other ground covers into second-time-period wheat pixels could degrade recognition performance substantially, depending on the spectral characteristics of the covers. For this data set, water had the greatest effect, followed by trees, soybeans, and corn in that order, with corn having very little effect. It also was shown that wheat false alarms could be markedly increased by misregistration. Misregistered tree pixels were most affected, followed by soybean, corn, and water misregistered pixels.

For further analysis, the following recommendations are made:

(1) Repeat the analysis of CITARS data, using a more compact set of signatures determined by editing the data prior to signature formation.

(2) Apply the same effort as described in this report to multitemporal LACIE data in order to examine effects of misregistration in the LACIE context.

(3) Expand the analysis to examination of more than two time periods and possibly more than one mixture crop.

(4) Consider improved approximations of between-time-period correlations for spatially misregistered pixels.

(5) Derive an analytical solution for that value of α (if any) for which a particular linear decision surface is crossed by a distribution of misregistered pixels.

(6) Given a fixed set of crop classes with associated signatures, simulate a corresponding multitemporal data tape and, for varying degrees of misregistration, actually perform recognition processing to examine recognition curves.

(7) Examine actual data sets registered by two or more different algorithms to determine which algorithm best controls registration so as to minimize misregistration effects and any performance penalty associated with the current LACIE procedure.

4
MULTITEMPORAL RECOGNITION STUDIES

The key part of any computer recognition processing effort is the training procedure used to establish signatures for the recognition operation, i.e., for the assignment of individual pixels to the various classes. Training procedures can be optimized or improved through an understanding of the physical and/or biological characteristics which determine the reflectance properties of crops. In this section, analyses of the spectral and multitemporal characteristics of signatures are described, as well as recognition processing results obtained with several different sets of signatures.

4.1 MULTITEMPORAL SIGNATURE CHARACTERISTICS

The multitemporal signatures considered in this section are from LANDSAT data sets that are collected weeks or months apart over the same site, in other words, data that are collected at various stages of vegetation growth (or phenological cycle). The objective is to utilize the added dimension of temporal information to improve upon single-time crop recognition and information extraction from scanner data. Although some results have been obtained with multitemporal data at various institutions, the multitemporal approach is one which requires additional research and development.

The temporal characteristics of crop signatures obtained in two different ways from CITARS data sets were examined. Primarily corn and soybean signatures were considered. The first approach was to extract

signatures for individual fields from data for several time periods. The second was to cluster pixels in a multitemporal data set. The characteristics of the two types of signatures were compared.

One reason for using the two approaches was that ground 'truth' information, consisting of periodic ground observations, was available for individual training fields. Data clustering techniques, on the other hand, can be independent of specific field boundaries . A greater understanding of signature characteristics can be obtained by analyzing both types of data.

Another way of examining the temporal characteristics of signatures is through simulation modeling. Some initial modeling work was performed for wheat signatures using a vegetation canopy reflectance model and a radiative transfer model to simulate atmospheric effects.

4.1.1 ANALYSIS OF INDIVIDUAL FIELD SIGNATURES

One point that is clear from the CITARS data sets [1] is that there can be substantial variation in the development stages of some crops at a given calendar time and consequent differences in their temporal appearance. Soybeans is perhaps the most notable example in that data set. Table 2 lists ground observations of characteristics of several selected soybean fields in Fayette County, Illinois, at seven times throughout the 1973 growing season. These times correspond to LANDSAT-1 passes over the segment. It can be seen that, while soybean fields follow the same maturation cycle, there are differences both in starting times and in total lengths of cycles. For example, Field 64-63 is one of several in the segment which were planted

[1] Malila, W. A., D. P. Rice, and R. C. Cicone, "Final Report on the CITARS Effort by the Environmental Research Institute of Michigan", Report No. NASA CR-ERIM 109600-12-F, Environmental Research Institute of Michigan, Ann Arbor, Michigan, February 1975.

TABLE 2. PHYSICAL AND BIOLOGICAL CHARACTERISTICS OF SELECTED SOYBEAN FIELDS, FAYETTE COUNTY, ILLINOIS, 1973

Characteristic	Field / Date	VALUE FOR INDICATED FIELD: 35-13	44-12	55-43	64-63	69-41	69-49	88-66
Height (inches)	Jun 10/11*	3	2	3	0	0	0	0
	Jun 29/30*	10	6	8	1	6	6	4
	Jul 16/17*	24	10	20	4	12	12	12
	Aug 3/4	30	30	30	12	30	30	26
	Aug 21/22*	36	36	40	22	36	38	38
	Sept 8/9	36	36	40	26	36	38	38
	Sept 26/27	0	36	40	28	36	38	38
Ground Cover (%)	Jun 10/11	0-5	0-5	0-5	Bare	0-5	0-5	Bare
	Jun 29/30	5-20	5-20	0-5	0-5	5-20	5-20	0-5
	Jul 16/17	80-100	20-50	20-50	0-5	20-50	20-50	20-50
	Aug 3/4	80-100	80-100	80-100	5-20	50-80	50-80	80-100
	Aug 21/22	80-100	80-100	80-100		80-100	80-100	90-100
	Sept 8/9	50-80	80-100	80-100	80-100	80-100	80-100	80-100
	Sept 26/27	0	80-100	80-100	80-100	80-100	80-100	80-100
Stage of Maturity (See Below)	Jun 10/11	1	1	1	0	0	0	0
	Jun 29/30	1	1	1	1	1	1	1
	Jul 16/17	2	1	1	1	1	1	1
	Aug 3/4	2	3	2	1	3	3	3
	Aug 21/22	4	3	4	2	3	3	3
	Sept 8/9	5	5	5	3	5	5	5
	Sept 26/27	21	6	6	5	5	6	6

*ERTS-1 coverage obtained

Stage of Maturity Key:

1 = Pre-bloom
2 = Blooming
3 = Early Pod Set
4 = Late Pod Set
5 = Turning yellow, leaves dropping
6 = Mature
21 = Harvested

late or replanted because of excessive wetness or replanted to soybeans after wheat harvest. Field 64-63 had very little ground cover (0-5%) in July, when a fast-growing field (like 35-13) had 80-100% ground cover and already was blooming. By the end of September, Field 35-13 was the only one of those listed that had been harvested, because others were slower in maturing.

Note also that only three of the seven fields listed were blooming (Maturity Stage 2) at the time of a LANDSAT-1 pass, one blooming as early as mid July and another as late as late August. The other four fields apparently bloomed in late July between LANDSAT-1 passes. The late-pod-set stage (#4) of soybean crop development also was missed by LANDSAT-1 in several fields. The conclusion must be for this set of data that the LANDSAT-1 system, with its 18-day cycle, undersamples the growth cycle of soybeans. Whether or not this precludes reliable recognition of soybeans over large areas under a variety of conditions remains to be seen.

The item of prime interest is how much the physical and biological differences between soybean fields affect their remotely sensed signatures and subsequent recognition. Cloud-free LANDSAT-1 data were collected over the Fayette segment for four time periods during the 1973 growing season -- early and late June, mid July, and late August. A spectral plot of temporal paths of field signature means is presented in Fig. 7 for the fields listed in Table 2. The plot is for LANDSAT Band 7 vs. Band 5 (digital channels 4 vs. 2). The paths start at the right in early June and progress generally to the left and upward as the season advances and ground cover increases.* Signatures were available at all four times for all except Field 35-13.

*Included in these changes are those due to changing sun angle and atmospheric state, and any instrumental changes, between time periods. It is possible but not considered likely that atmospheric or instrumental differences existed within a single time period for the data analyzed.

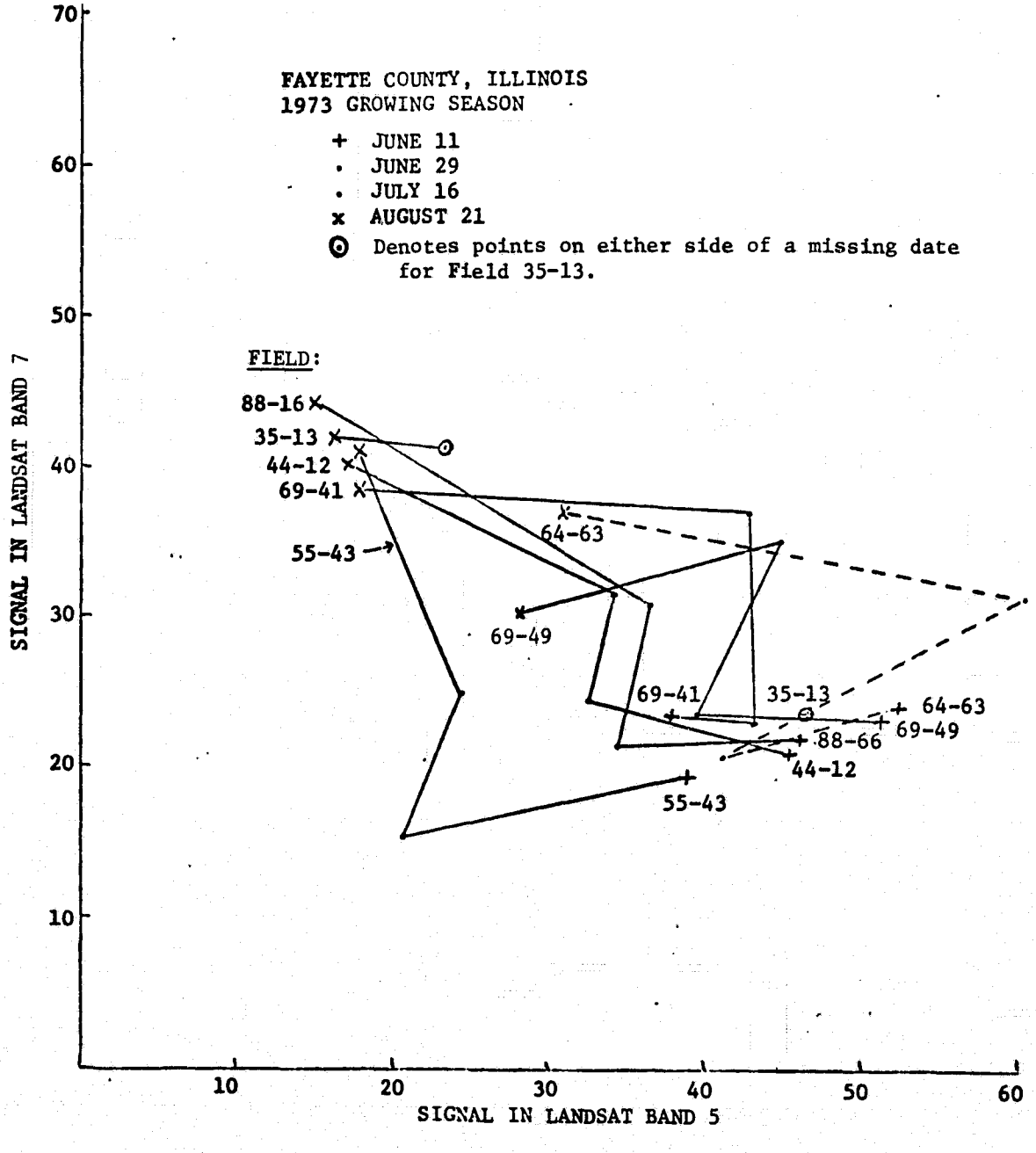

FIGURE 7. TEMPORAL PATHS OF LANDSAT SIGNATURE MEANS FOR SOYBEAN FIELDS

June 29th data are missing for this field. Correlations between signature location and crop cover can be seen by comparing Table 2 with Fig. 7.

4.1.2 ANALYSIS OF MULTITEMPORAL CLUSTER SIGNATURES

The clustering algorithm and procedure used to determine the signatures analyzed in this section are described in Sec. 4.2.1. Briefly, the data set analyzed contained LANDSAT-1 data from four time periods over the CITARS Fayette segment (10 June, 29 June, 17 July, and 21 August 1973). Eight of the 16 channels of multitemporal data were used in the clustering procedure -- data channels 2 and 4 (LANDSAT Bands 5 and 7) from each time period. Labels assigned to the training pixels prior to clustering were used to identify the various clusters.

A total of 21 clusters was defined from field-center pixels of training data -- 12 for soybeans, three for corn, and six for "other". These remained after a combination was made of 33 clusters found at an intermediate stage. As an aid for analysis on this and other tasks, a computer program was written to generate a variety of graphical representations of signatures.

Two types of plots were made of the statistics of the clusters obtained. One type is a plot of means plus or minus one standard deviation as a function of time for each of the 33 intermediate clusters . Fig. 8 presents plots for the largest three of four corn clusters, seven of 22 soybean clusters, and five of seven "other"-class clusters. The cluster labels are explained in Table 3. The x-axis is a time axis, and the first four points represent signals in LANDSAT Band 5 (0.6 - 0.7 μm) with the earliest time on the left and latest on the right. The last four points similarly represent signals in LANDSAT Band 7 (0.8 - 1.1 μm).

FIGURE 8. MAJOR MULTITEMPORAL CLUSTERS, FAYETTE SEGMENT
(Part 1 of 3)

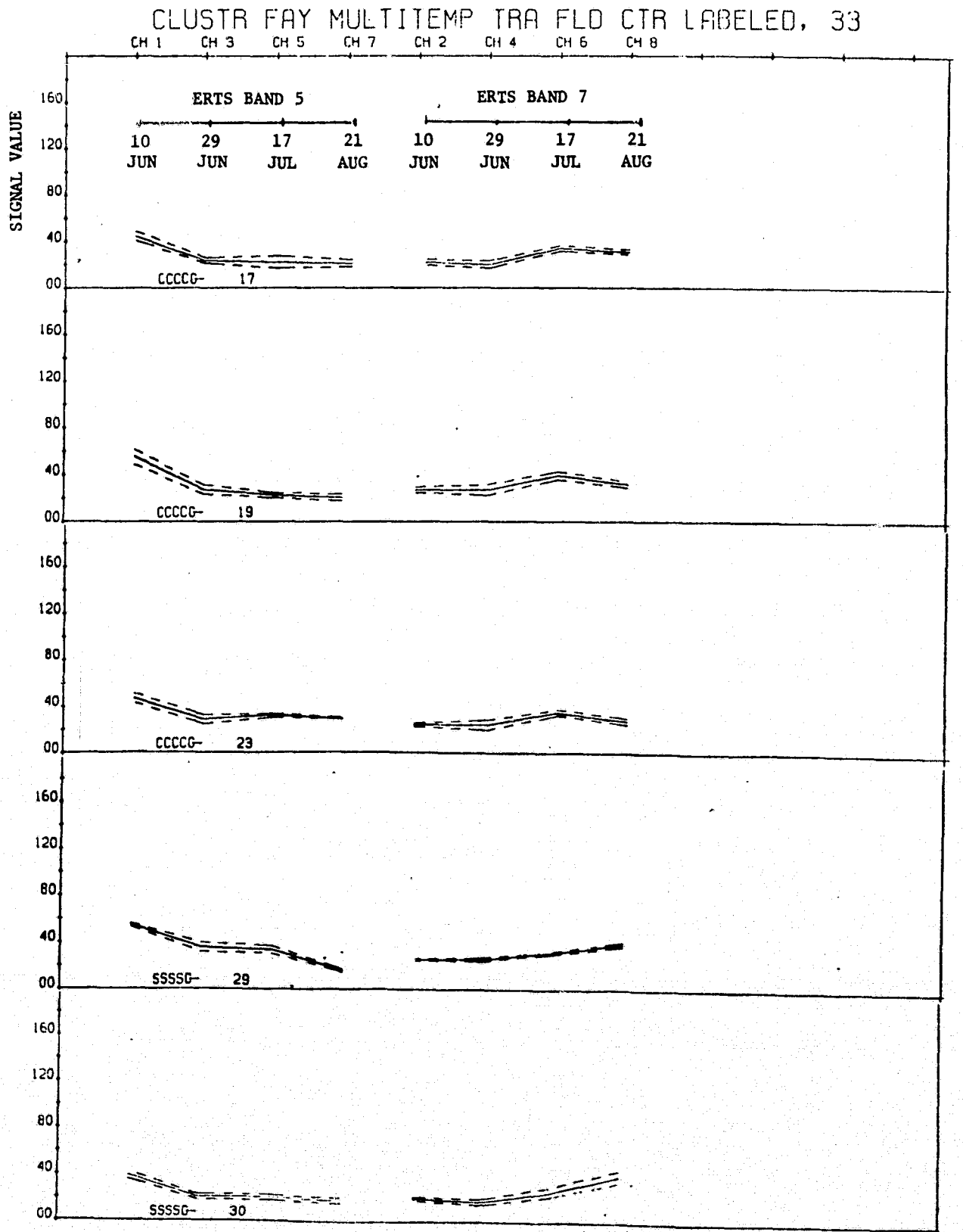

FIGURE 8. MAJOR MULTITEMPORAL CLUSTERS, FAYETTE SEGMENT
(Part 2 of 3)

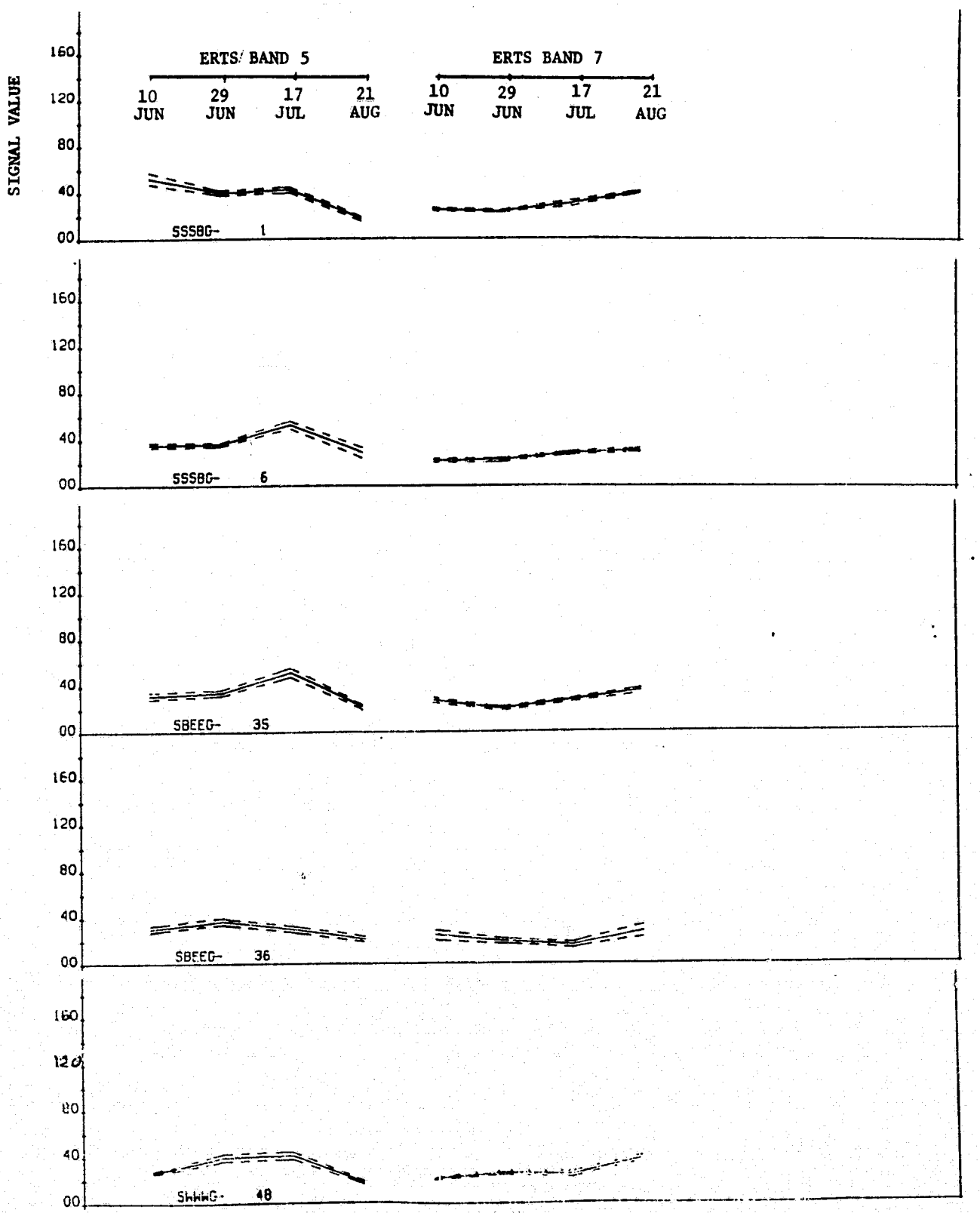

FIGURE 8. MAJOR MULTITEMPORAL CLUSTERS, FAYETTE SEGMENT
(Part 3 of 3)

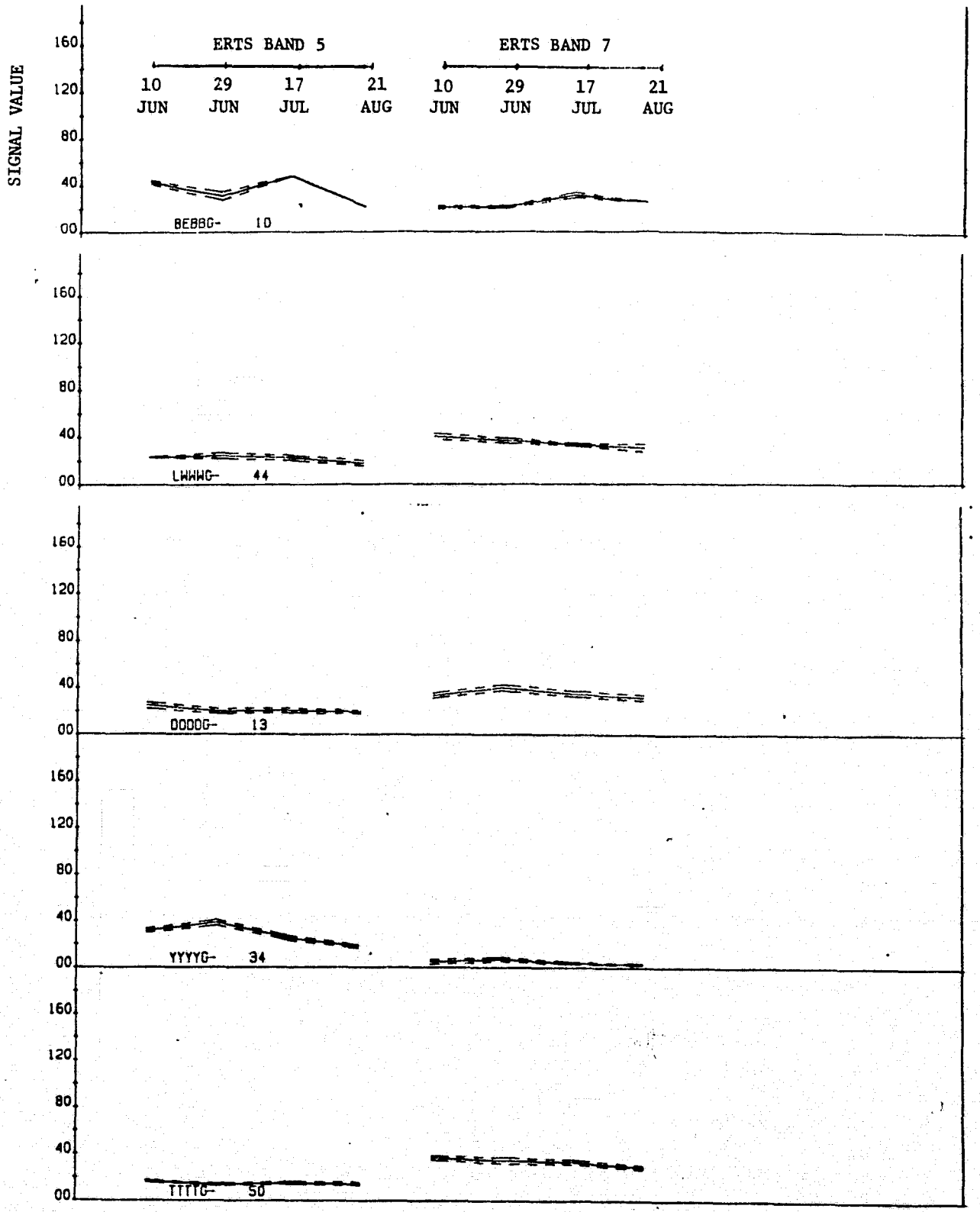

TABLE 3. DEFINITION OF CLUSTER LABELS

CHARACTER CODE:

C	-	corn
S	-	soybeans
B	-	bare soil
E	-	weeds
W	-	wheat
L	-	clover
U	-	legume
D	-	brush
Y	-	water
T	-	trees

LABEL DESCRIPTION:

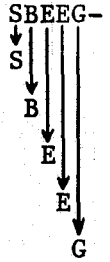

Denotes soybeans on 21 Aug. (ERTS Cycle V)

Denotes bare soil on 17 Jul (ERTS Cycle III)

Denotes weeds on 29 Jun (ERTS Cycle II)

Denotes weeds on 11 Jun (ERTS Cycle I)

Denotes training field

Note that the latest date is represented by the left-most character in the label whereas the latest date is right-most on the time plots of Fig. 8.

The plots of Fig. 8 portray both the multitemporal differences between classes and the variability within the soybean class; the greater number of soybean clusters is another indication of this variability. One notable common characteristic of the soybean plots is their increase in Band 7 values from 17 Jul to 21 Aug and the corresponding decrease in Band 5 values between the same times. This characteristic is related to their increasing percentage of ground cover as the season progresses, leading to higher infrared reflectances and lower red reflectances. Corn also had increasing ground cover, but generally reached maturity faster than soybeans and had tasseled by 21 August. Water (Y) and tree (T) cluster plots also are interesting. There is little temporal change in the tree signature, but the water signals seem to be correlated with the maximum sun elevation angle throughout the period, i.e., the maximum signal is found for 29 June, the time nearest the summer solstice.

The second type of plot generated was of two-dimensional ellipses which represent two-channel signatures of various fields, clusters, or crops. The center of each ellipse represents the mean of the signature, while the size and shape of the ellipse are determined by the variance-covariance matrix, i.e., by both the correlation between the two channels and the relative magnitudes of their variances. For perfect correlation, the ellipse would collapse to a straight line skew to the coordinate axes while, for zero correlation, the axes of the ellipse would be aligned with the coordinate axes. The size of the ellipse is a function of both the variances and the χ^2 level chosen for the display. The χ^2 level is a measure of the squared distance from the mean in covariance units, and the ellipses

presented here are for $\chi^2 = 1$. For two degrees of freedom, approximately 40% of the points from a bivariate normal distribution would lie within such an ellipse.

In order to make a comparison with the temporal paths of individual soybean fields in Fig. 7, ellipses were plotted in Fig. 9 for several soybean clusters at each time period. A two-part number is associated with each ellipse -- the first part identifies the cluster and the second the time period (1-4) . The general pattern is the same as found in Fig. 7. In the first time period, most had bare-soil signatures, which incidentally cover quite a range of soil colors (the lighter the soil, the farther from the origin is the ellipse). One exception was Cluster 11 which corresponds to pixels that were weeds in time periods one and two; they apparently were not planted to soybeans until just before time period three when these pixels exhibited a bare soil response. Cluster 10 had the greatest number (37.0%) of soybean pixels; Clusters 4 and 5, which followed quite similar paths, had 3.4% of the soybean pixels each. Cluster 11 had 8.9%. Cluster 6 apparently represents the fastest growing and maturing soybeans, approximately 4.1% of the soybean pixels analyzed.

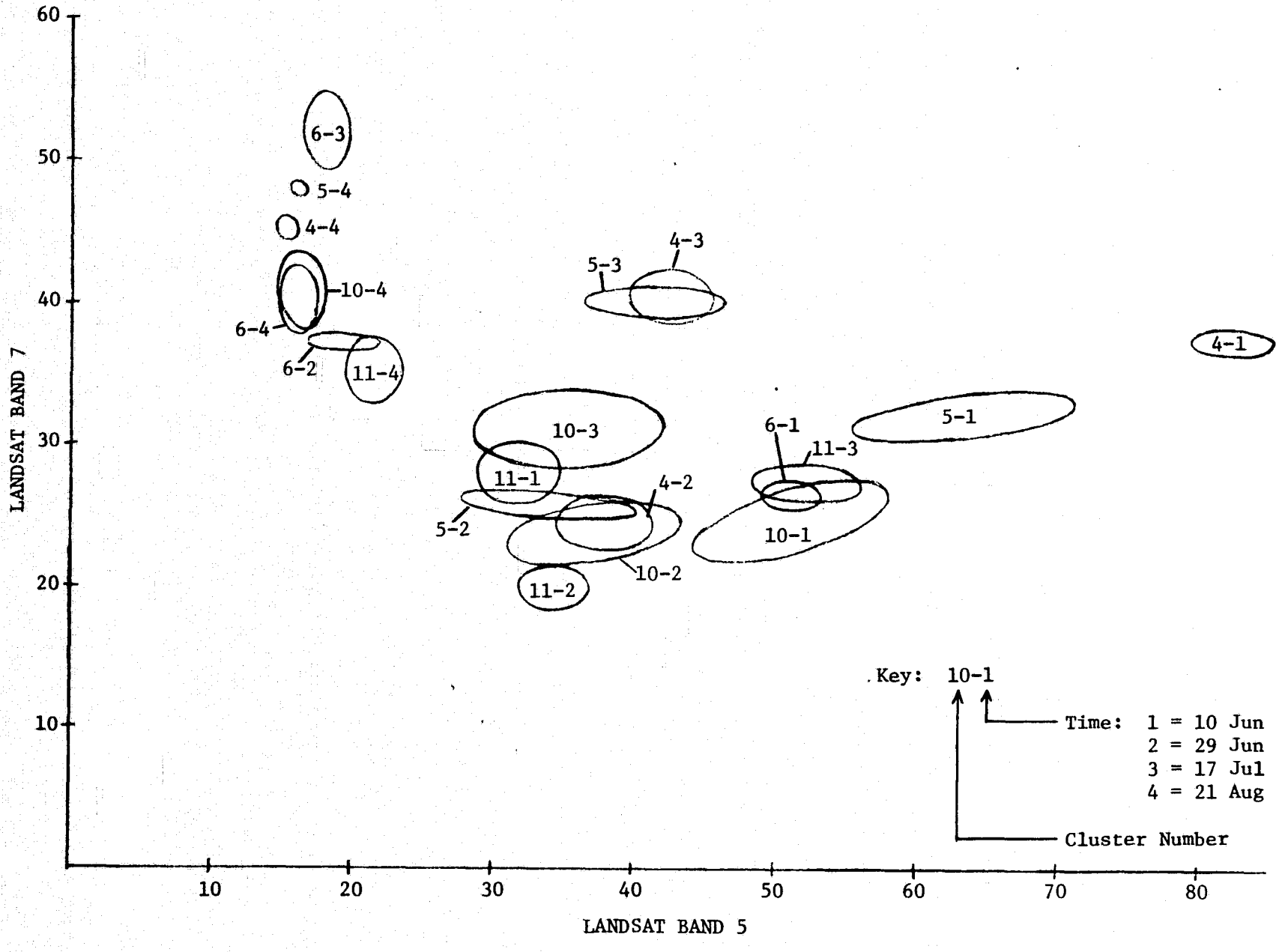

FIGURE 9. TEMPORAL PATTERNS OF SELECTED SOYBEAN CLUSTERS

4.1.3 SIMULATION OF SIGNATURES

A simplified equation for the radiance L at a satellite from a vegetation canopy is:

$$L = \rho_c \frac{ET}{\pi} + L_p$$

where ρ_c is the diffuse reflectance of the vegetation canopy,

E is the solar and sky irradiance on the canopy,

T is the transmittance of the atmosphere between target and sensor,

and L_p is extraneous path radiance.

In order to simulate a multispectral signal at a satellite, one must calculate or represent both the reflectance of the vegetation canopy and effects (T, L_p, and E) of the atmosphere and the sun at wavelengths of interest. These surface and atmospheric quantities are not completely independent. First, they are linked by the geometry of observation relative to the sun's position. Second, E and L_p depend on both the amount of haze in the atmosphere and on the reflectance (albedo) of the background in which the target material is located. Yet, one can benefit from separate studies of canopy reflectances and atmospheric effects before the two are combined to simulate signals.

A canopy of vegetation such as wheat is composed of components -- various kinds of leaves, stalks or tillers, heads, and the underlying soil . As the plants emerge from bare soil, grow, and mature, there are changes in the relative contribution of each component to the reflectance of the canopy. These are determined by the structural properties of the canopy and the reflectance and transmittance properties of each component. Dr. Gwynn Suits of ERIM was the first to develop a reflectance model for vegetation

canopies that took into account these factors and the observation and solar geometries to computer reflectances with directional properties [5]. He and collaborators G. Safir and M. Weiss made physical measurements of wheat components, computed field reflectances with the model, and confirmed the calculations with measurements of wheat field reflectances [6].

Calculations of wheat field reflectances were made with the Suits model at several growth stages for several different soil colors. Wheat component reflectances, transmittances, and canopy parameters measured in Michigan by Safir, et al, for Ionia wheat were used for one set of calculations. Another set was made by substituting reflectance and transmittance values measured by Wiegand, et al, at Weslaco, Texas, [7] for healthy green leaves. There are substantial differences in these two reflectance measurements, quite possibly linked with varietal differences or perhaps due to measurement procedure differences. The Weslaco wheat tended to have higher leaf reflectance values and lower absorptances.

Results of the reflectance calculations for one soil type and the two varieties are presented in Fig. 10(a). The two varieties have essentially equal reflectances at both the emergent stage (1) and the senescent stage (4). However, the differences in green leaf characteristics are very evident in stages 2 and 3 of the wheat canopy. (Stage 3.5 was arbitrarily defined to have half green and half chlorotic leaves.)

---

[5] Suits, Gwynn H., 1972. "The Calculation of the Directional Reflectance of a Vegetative Canopy", Remote Sensing of Environment, Vol. 2, pp. 117-125.

[6] Safir, G. R., G. H. Suits, and M. V. Weiss, 1972. "Applications of a Directional Reflectance Model to Wheat Canopies Under Stress", Proceedings of International Conference on Remote Sensing in Arid Lands, Tuscon, Arizona, Nov. 9, 1972.

[7] Wiegand, C. L., et al., 1971. Spectral Survey of Irrigated Region Crops and Soils, 1971 Annual Report, Weslaco Agricultural Research Center, U.S. Department of Agriculture, Weslaco, Texas, December 1971.

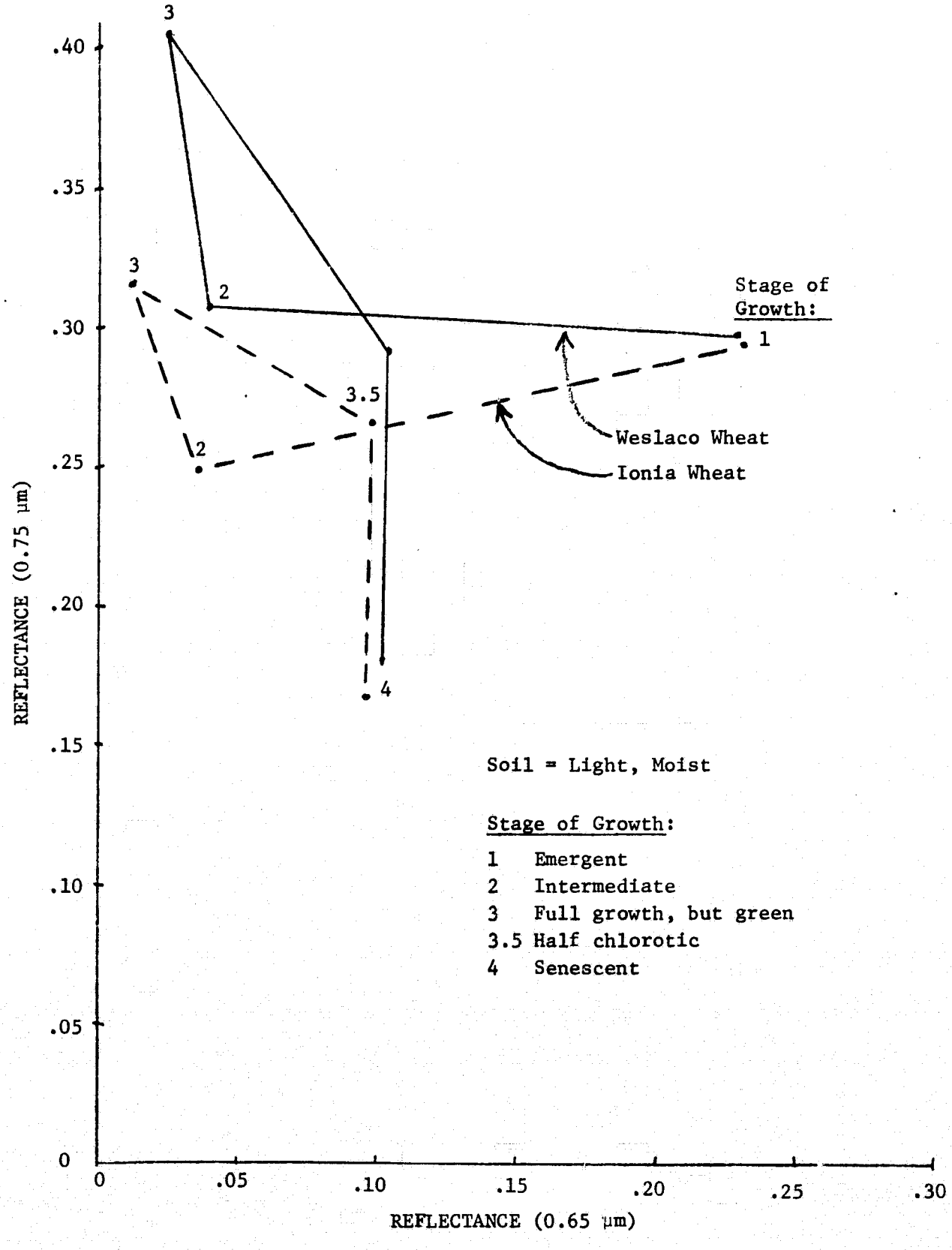

(a) INFLUENCE OF WHEAT LEAF CHARACTERISTICS

FIGURE 10. CALCULATED MULTITEMPORAL REFLECTANCES FOR WHEAT (Continued)

Fig. 10(b) illustrates the effect of soil color on wheat canopy reflectances for one variety. A light soil was considered for three moisture conditions -- dry, moist, and wet -- along with a dark soil. The range of soil reflectances is evident in the stage-1 values. A very striking feature of this figure is that reflectances for stages 3, 3.5, and 4 are independent of soil color. This is due to the high ground cover percentages (mid 90's) used for these mature stages.

Calculations also were made for two view (scan) angles, 0^{o} and 4^{o} off nadir. The results showed little scan-angle dependence at 550 nm (except for stage 2) but progressively more in longer-wavelength LANDSAT bands, with a maximum change of 8% of the nadir value. The values plotted in Fig. 10 are for a scan angle of 4^{o} and a solar zenith angle of 28^{o}.

These calculations should be considered to be preliminary and exploratory in nature because of the scarcity of measured data on wheat reflectance, transmittance, and canopy structure characteristics, especially for the varieties and conditions of wheat in the major wheat-producing areas. Yet, some possibly significant sources of variation have been identified. It is recommended that such characteristics be measured as part of the field measurement program for wheat during the 1975 growing season.

The other aspect of simulation is to account for atmospheric effects. We use the radiative transfer model developed by Dr. Robert Turner at ERIM [8]. With it one can compute the surface irradiance as a function of solar zenith angle, haze content, and surface albedo. Also, the path radiance and atmospheric transmittance are calculable as functions of the same quantities

[8] Turner, R. E., "Atmospheric Effects in Remote Sensing," Selected Papers from the March 26-28, 1973, Remote Sensing of Earth Resources Conference, Vol. II, ed. F. Shahrokhi, University of Tennesseee Space Institute, Tullahoma, 1973.

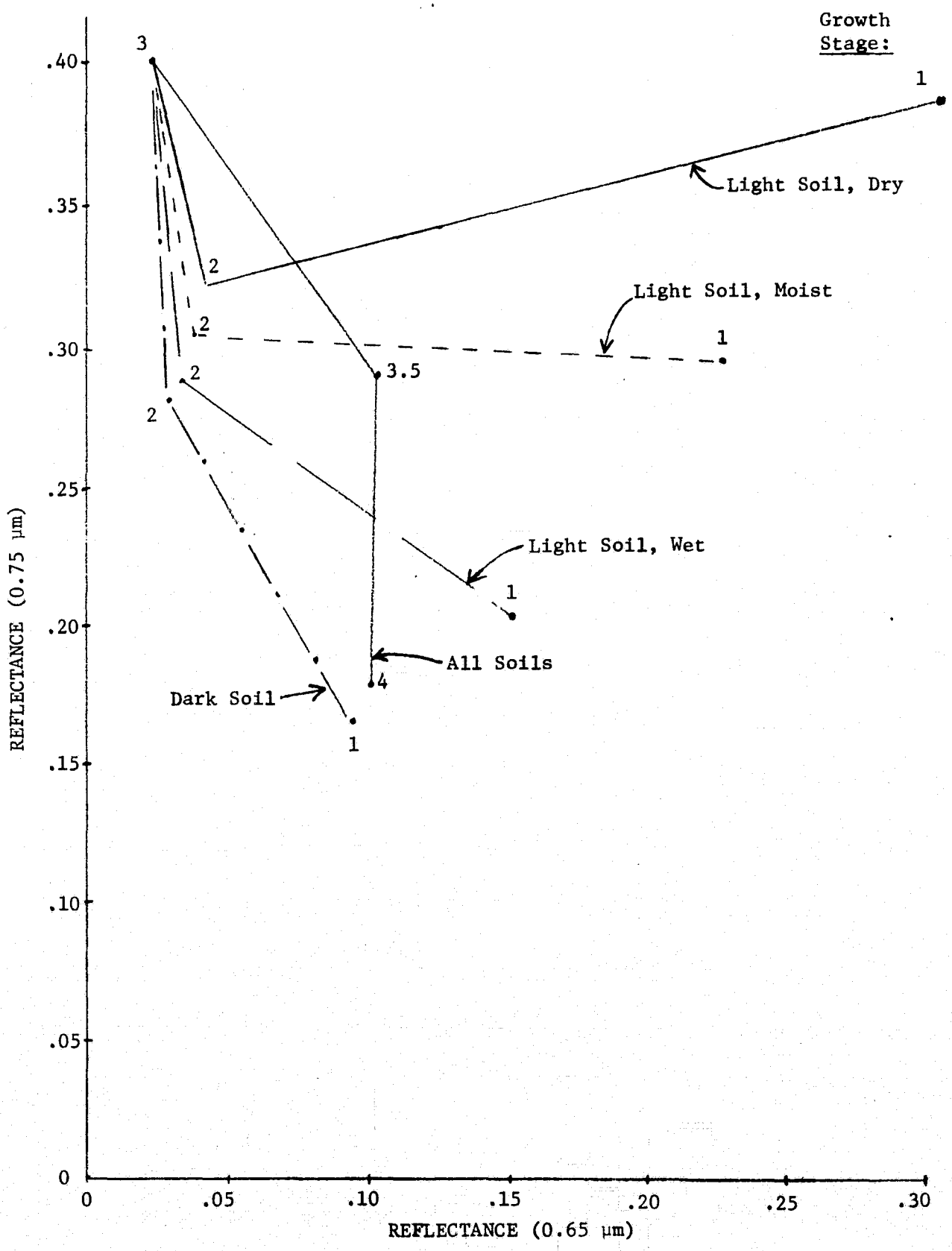

(b) INFLUENCE OF SOIL COLOR

FIGURE 10. CALCULATED MULTITEMPORAL REFLECTANCES FOR WHEAT (Concluded)

plus the scan angle and azimuth angle difference between the sun and view directions. Specific calculations are not presented in this section, because the general characteristics are discussed quite fully elsewhere, Refs. 8 and 9, for example.

---

[8] Turner, R. E., "Atmospheric Effects in Remote Sensing, Selected Papers from the March 26-28, 1973, Remote Sensing of Earth Resources Conference, Vol. II, ed. F. Shahrokhi, University of Tennessee Space Institute, Tullahoma, 1973.

[9] Turner, R. E., W. A. Malila, R. F. Nalepka, and F. J. Thomson, "Influence of the Atmosphere on Remotely Sensed Data", Proceedings of SPIE Seminar on Scanners and Imagery Systems for Earth Observation, August 1974.

4.2 MULTITEMPORAL RECOGNITION PROCESSING

There are a number of parameters and procedures that can be varied during recognition processing of multispectral scanner data. The approach taken here with multitemporal data from CITARS was to vary some parameters (rejection threshold, number of signatures, and amount of training data) in a relatively systematic way to determine the sensitivity of results to these parameters, as well as to obtain a better understanding of the maximum attainable recognition performance.

CITARS LANDSAT data from four time periods over the Fayette segment (10 June, 29 June, 17 July, and 21 August 1973) were merged to form a multitemporal data tape. These data previously had been placed in spatial registration by Purdue/LARS as part of the CITARS data preparations; a nearest-neighbor algorithm was used for interpolating to obtain values on the reference grid. Two other passes also were available but were not used because each was within one day of one of the selected passes; furthermore, clouds were present on 11 June and the 16 July data set had some data quality problems. The 29 June data set was included despite a number of bad data lines since, otherwise, the late June time period would not be represented.

4.2.1 TRAINING PROCEDURES

Data clustering was used to determine several sets of recognition signatures. It was first used on labeled field-center pixels from ASCS-identified fields. (ASCS is the Agricultural Stabilization and Conservation Service of the U.S. Dept. of Agriculture.)

The intersection of pixel assignments for the four time periods was used to define a subset of the field-center pixels of ASCS-visited areas that had been identified for training in the CITARS data preparations. This subset excluded fields that had data problems at one or more time periods. Four-character labels were assigned to the pixels of each field, one character to represent the ground-truth class at each of the time periods. There was only one label for all the corn pixels, but four different types of labels were needed to represent the variety of soybean planting dates and maturities.

The pixel-by-pixel clustering algorithm used to establish a set of clusters from the field-center training pixels is documented in Ref. 10. One feature of the algorithm is a capability to label pixels and use that labeling in the clustering procedure. Thus, one or more clusters was generated for each of the labeled classes. An iterative procedure was used to combine the many clusters generated on the only pass through the data into a smaller number for use in recognition. Another feature of the algorithm is its distance measure which accounts for the variances associated with the clusters as well as mean separations.

Only eight of the 16 channels of multitemporal data were used in the clustering procedure. A selection was made of data channels 2 and 4 (LANDSAT Bands 5 and 7) from each time period; although arbitrary, this selection was made in part because of the high degree of correlation that has been observed between channels 1 and 2 and between channels 3 and 4.

---

[10] Horwitz, H., J. Lewis, and A. Pentland, "Estimating Proportions of Objects from Multispectral Scanner Data", Report No. 109600-13-F, Environmental Research Institute of Michigan, Ann Arbor, Michigan, March 1975.

The 21 signatures discussed in Sec. 4.1.2 were established from the ASCS data. These were used for recognition processing of test data that had been "ground truthed" by photointerpreters from multitemporal aerial photography. Results of the recognition operations are presented and discussed in the next section, but we here note that several soybean fields were completely missed, that is, were not assigned to any of the 21 signatures.

An augmented signature set was established by adding two new soybean clusters obtained by applying the clustering procedure to six of the test fields that were completely missed. Recognition processing was performed again.

Finally, all field-center pixels (both ASCS- and PI-identified) were clustered using the previously described procedure. (Only seven channels were used because of uncertainties about possible bad line problems in PI-identified fields for Channel 4, 29 June.) This resulted in 49 clusters. Recognition runs were made both with 49 signatures and with a subset consisting of the 30 with the largest number of pixels assigned in the clustering operation. These runs were designed to estimate an upper bound on the recognition performance that might be attained for this data set.

4.2.2 RECOGNITION RESULTS FOR FIELD CENTERS

Although training on ASCS fields was conducted on eight channels, recognition was performed with only seven, because of possible problems with bad lines in channel 4 for 29 June.

Recognition results with the 21 clusters, seven multitemporal channels, and the ERIM linear decision rule were obtained for five different decision thresholds and the original CITARS-defined test pixels. The thresholds correspond approximately to 0.001, 0.0003, 0.0001, 0.00001, and 0^+ probability of falsely rejecting a point from the assumed multivariate normal signature distributions.

Corn recognition was 94.8% for all threshold values. Fifteen corn pixels were missed on each run. At the 0.001 threshold, eleven of these were rejected and four assigned to an incorrect class while, at the other extreme of threshold, only three were rejected and 12 were assigned to an incorrect class . The number of non-corn pixels falsely recognized as corn rose from 24 at 0.001 threshold to 69 for 0^+ threshold.

Soybean recognition ranged from 72.1% to 91.3% correct, depending on threshold. None of the missed soybean pixels were falsely assigned to another recognition class; all were rejected by the threshold test but, nevertheless were considered to be assigned to class "other" for purposes of recognition performance calculations. This fact indicates that the training data were not fully representative of the soybean test fields.

Recognition of the "other" class was 86.1% correct for the 0.001 threshold and decreased monotonically as the rejection threshold approached zero, reaching a value of 64.2% correct for 0^+ threshold.

The overall percentage of points correctly recognized was largest (84.6%) for the 0.0003 rejection threshold, as shown in Table 4. This threshold value also was best with the augmented signature set discussed in the next paragraph .

TABLE 4. MULTITEMPORAL RECOGNITION RESULTS ON FAYETTE TEST FIELD CENTERS. (Using CITARS-defined test fields)

APPROXIMATE REJECTION THRESHOLD		0.001	0.0003	0.0001	0.00001	0^+
Parameter EXPLIM		24	27	30	35	511
TEST FIELD % POINTS CORRECT:*	Total # Points					
CORN	286	94.8	94.8	94.8	94.8	94.8
SOYBEANS	358	72.1	77.1	78.8	81.6	91.3
OTHER	374	86.1	84.0	80.5	77.3	64.2
AVG. OVER POINTS	1018	83.6	84.6	83.9	83.7	82.3
TEST FIELD POINTS MISSED: (REJECTED/MISCLASSIFIED)						
CORN		11/4	9/6	8/7	7/8	3/12
SOYBEANS		100/0	82/0	76/0	66/0	31/0
FALSE DETECTIONS TO:						
CORN		24	28	34	39	69
SOYBEANS		28	33	40	47	68
OTHER		115	96	90	80	43
TOTAL		167	157	164	166	180

Notes: (1) 21 clusters from training data.

(2) 7 of 8 multitemporal data channels; channel 4 (LANDSAT Band 7) omitted for 29 June, because of bad scan lines.

*Larger values result when several known errors in the test pixel labels are corrected -- see Table 5.

Because of the previously noted failure of the signatures to recognize pixels from a number of soybean fields, it was decided to augment the soybean signatures with others determined from six fields that were completely missed with the 0.001 threshold (these represent 43 of the 100 soybean pixels missed at that threshold). The pixels from these fields were clustered and two new soybean signatures were established. Table 5 shows an improvement in soybean recognition from 77% to 84% when this additional pair of signatures was used with a 0.0003 threshold. Still, 56 soybean pixels remained unclassified, i.e., rejected by the threshold test.

A careful examination and comparison was made of field-center pixel definitions and associated "ground truth" information, in a joint analysis of Fayette 21 Aug CITARS data by several tasks on this contract. A number of discrepancies were found and corrected. Several involved the wrong crop ID, several the inclusion of two or more dissimilar ground covers in one field definition, and a few the inclusion of very atypical growth patterns as test fields for evaluation. Details of the corrections are presented in Sec. 6 of Ref. 1. Results also are presented in Table 5 for corrected field definitions, for comparison with those with the standard CITARS field definitions. An improvement of 1.4% to a new result of 88.5% correct is realized with these changes.

As a further demonstration of the need for more representative training data and as an estimate of the maximum achievable recognition accuracy on this data set, recognition runs were made using the signatures based on all field-center pixels. As shown in Table 6, results of runs with 49 signatures showed that overall field-center accuracy increased to 94% correct,

---

[1] Malila, W. A., D. P. Rice, and R. C. Cicone, "Final Report on the CITARS Effort by the Environmental Research Institute of Michigan", Report No. NASA CR-ERIM 109600-12-F, Environmental Research Institute of Michigan, Ann Arbor, Michigan, February 1975.

TABLE 5. EFFECTS OF TWO ADDED SOYBEAN SIGNATURES AND CORRECTED FIELD DEFINITIONS ON MULTITEMPORAL RECOGNITION, FAYETTEE SEGMENT

	ORIGINAL CITARS FIELD DEFINITIONS		REVISED FIELD DEFINITIONS
	TRAINING-FIELD CLUSTERS ONLY	WITH TWO SUPPLEMENTAL SOYBEAN CLUSTERS	WITH TWO SUPPLEMENTAL SOYBEAN CLUSTERS
TEST FIELD CENTERS, % POINTS CORRECT:			
CORN	94.8	94.8	94.8
SOYBEANS	77.1	84.4	84.9
OTHER	84.0	84.4	86.6
AVG. OVER POINTS	84.6%	87.1%	88.5%
TEST FIELD POINTS MISSED: (REJECTED/MISCLASSIFIED)			
CORN	9/6	14/1	9/6
SOYBEANS	82/0	56/0	54/0
FALSE DETECTIONS TO:			
CORN	28	28	27
SOYBEANS	33	33	10
OTHER	96	70	68
TOTAL	157	131	105

NOTES: (1) 0.0003 rejection threshold

(2) 7 channels

(3) 21 signatures based on training field clusters

(4) The test pixels used are the revised CITARS field-center set with urban pixels retained (See Table 12, Ref. 1).

TABLE 6. MULTITEMPORAL RECOGNITION RESULTS FOR TRAINING ON ALL FIELD-CENTER PIXELS

TOTAL NUMBER OF SIGNATURES	TRUE CLASS	% PIXELS CORRECT	TOTAL NO. PIXELS	TEST PIXELS RECOGNIZED AS: CORN	SOYBEAN	OTHER
30	CORN	90.6%	286	259	2	25
	SOYBEANS	92.2%	357	0	329	28
	OTHER	95.2%	269	11	2	256
		92.5%	912			
49	CORN	89.2%	286	255	5	26
	SOYBEANS	96.1%	357	0	343	14
	OTHER	96.3%	269	10	0	259
		94.0%	912			

NOTES: (1) Threshold for 0.0003 probability of false rejection.

(2) The test pixels used are the revised CITARS field-center set with urban pixels retained (See Table 12, Ref. 1).

(3) The 30 signatures are a subset of the 49.

with soybean accuracy increasing by nearly ten percentage points to a new value of 96.1% correct. Improvements for a subset consisting of the 30 largest-cluster signatures were nearly as great; for example, the overall accuracy improved to 92.5% correct as shown in Table 6. It is interesting to note that corn recognition accuracy decreased slightly as the number of clusters increased. The increase over the 23 clusters was primarily in the number of soybean clusters, i.e., 16 new ones for a new total of 30. There was an increase of two corn clusters giving a new total of five, and in increase of eight "other" clusters for a new total of 14.

It is worthy of note that the ERIM linear decision rule employed for multitemporal recognition processing affords a substantial savings in computer cost over the more conventional quadratic decision rule and, in other tests, has shown comparable recognition performance. The cost advantage gradually increases as the number of signatures used increases -- for four channels, the linear cost is about 1/3 the quadratic cost for four signatures and less than 1/4 for 50 signatures. The cost advantage of the linear rule also increases as the number of channels increases.

4.2.3 RECOGNITION RESULTS FOR FULL SECTIONS

Full-section recognition results do not depend on the accuracy with which field-center pixels can be located and identified, except for data used in training. Test data here included all pixels within square-mile sections and, thusly, included a variety of boundary and mixture pixels. The evaluation of these results consequently depends on "wall-to-wall"

ground truth so that the true proportions of all crops in each test section can be computed for comparison with the proportions recognized in multispectral scanner data.

Full-section results were obtained for the 49-signature multitemporal recognition run and are compared in Table 7 with results obtained using the standard ERIM CITARS procedures on Fayette 21 August single-time data. It so happens that soybean proportions were accurately and equally well recognized by both processing procedures. However, corn presented a much different situation, because the estimated proportion of corn for the single-time processing was nearly double the true amount and there was a large variance in estimates for individual sections. The corn proportions estimated from the multitemporal data were much more accurate, the overall corn proportion being almost exactly the same as the ground truth proportion and the variance in section estimates reduced to 1/4 of the single-time variance; however, variance in corn estimates still exceeded that for soybeans.

The RMS deviation in the last column of Table 7 is an overall measure of the residual bias in crop proportion estimates over the entire test area. This measure also indicates an excellent performance for the multitemporal procedure, as opposed to the single-time procedure.

4.3 CONCLUSIONS AND RECOMMENDATIONS

The use of seven-channel multitemporal data did increase recognition performance above that achievable with the best single-time data on the Fayette segment of CITARS data. The improvement in crop proportion estimates in full-sections was especially good.

TABLE 7. COMPARISON OF FULL-SECTION RECOGNITION RESULTS, FAYETTE SEGMENT

	CORN	SOYBEAN	OTHER	RMS DEVIATION*
GROUND TRUTH PROPORTION (%)	19.7	29.3	51.0	
CITARS RESULTS, 21 AUGUST				
Recognized Proportion (%)	36.8	28.6	34.6	13.7
RMS Error Between Sections (%)	19.98	6.38		
MULTI-TEMPORAL RESULTS				
Recognized Proportion (%)	19.6	26.8	53.6	2.1
RMS Error Between Sections (%)	9.51	6.16		

*Note that small values are best; values were computed as:

$$\text{RMS Deviation} = \sqrt{\frac{1}{n} \sum_{i=1}^{n} (p_i - \hat{p}_i)^2} \times 100\%$$

where p_i = true proportion of crop i in data set (from ground truth)

$\hat{p}_i$ = proportion of area recognized as crop i

n = number of crop classes

It was found that the ASCS-visited fields used for training in CITARS processing did not fully represent the variability of signatures found in test data, especially for soybeans which were planted at widely different times. When all available fields were used for both training and test, a field-center recognition accuracy of 94% correct was achieved.

The ERIM linear decision rule performed well in recognition processing of multitemporal data with a large number of signatures. Computer costs were three to four times less than they would have been with the more conventional quadratic decision rule.

Calculations of wheat field reflectances with a vegetation canopy reflectance model showed marked differences in values, differences attributable to the leaf reflectance and transmittance characteristics used. The only two sets of leaf measurements of which we are aware have quite different values, perhaps due to variety differences. Simulation modeling is a useful way of determining which factors are important in signature determination.

Several recommendations can be made, based on the studies reported herein. One would be to process and analyze LACIE data where wheat is more plentiful than in the CITARS data sets. Another would be to use only four information channels of multitemporal data in recognition processing for comparison with results with the four single-time channels. More generally, additional studies of both the multitemporal characteristics of signatures and procedures used for training is recommended, particularly for wheat and its confusion crops. It is recommended that wheat leaf reflectance and transmittance measurements be made for several varieties and conditions of wheat that are typical of the important wheat production areas, in addition to reflectance measurements of wheat fields.

5

TIME-OF-DAY STUDY WITH AIRCRAFT MSS DATA

Until recent years, multispectral remote sensing has been usable for extracting information only over very limited areas and during times involving essentially identical conditions. Training has been performed primarily on data from known ground areas under the same local conditions as the test data (the information so derived is generally called a "signature" for each ground cover). A major consideration of this contract effort was to understand time-of-day variations in signatures so remote sensing methods can be used to accurately extract ground information without the necessity to retrain locally for each variation in conditions. The work performed and reported here continued and concluded studies which were started under Task VI of the prior contract, as reported in Ref. 2.

5.1 INTRODUCTION AND REVIEW OF PRIOR WORK

Time-of-day variations include primarily changes in sun elevation and azimuthal angles, but also could include potential changes in atmospheric conditions and/or ground-cover conditions, such as leaf attitude changes, through the course of a day. This work used a unique data set collected over Ingham County, Michigan. Data were collected repeatedly over the same known ground-truthed area of varied agricultural crops and other vegetation at different times of day (from 9:33 AM through 2:50 PM Local Solar Time) on the same date (6 August 1971). This data set is particularly valuable in allowing one to study the effect of changes in time of day independently of parameters associated with different ground areas and/or seasonal changes. Other data sets which are available for differing times of day were collected over different

---

[2] Malila, W. A., R. H. Hieber, and J. E. Sarno, "Analysis of Multispectral Signatures and Investigation of Multi-Aspect Remote Sensing Techniques", Report NASA CR-ERIM 109100-27-T, Environmental Research Institute of Michigan, Ann Arbor, Michigan, July 1974.

ground areas and/or at different days of the season. While this data set was collected by aircraft from 1.52 km (5000 ft), the conclusions derived regarding differing times of day are expected to be applicable as well to Earth satellite data.

Possible approaches to studying and compensating for time of day or other variations in multispectral signatures can be broken into three general phases -- first, empirical studies of the changing remotely sensed signals caused by variations in each condition; second, theoretical calculations of the expected changes; and, third, empirical measurements of the improvement in recognition accuracy made possible by applying the information obtained from either or both of the first two phases to correct the training information for changing conditions.

Under last year's effort, work was essentially completed on the first two phases for this data set. In addition, recognition accuracy was shown to be seriously degraded when signatures from the first run were applied to later runs without adjustment. Analysis pointed to a pass-to-pass calibration problem in one of the channels. It was believed to be important both to repeat the recognition performed last year, avoiding the calibration problem, and to apply a few procedures for adjusting signatures and compare their ability to improve recognition at differing times of day, applying some of the information gained from the first phases. Another effort under this sequence of contracts is working primarily on developing signature extension techniques [11, 12] and has analyzed other data sets.

---

[11] Vincent, R., G. Thomas, and R. Nalepka, "Signature Extension Studies", Report No. 190100-26-T, Environmental Research Institute of Michigan, Ann Arbor, Michigan, July 1974.

[12] Henderson, R. G., G. S. Thomas, and R. F. Nalepka, "Methods of Extending Signatures and Training Without Ground Information", Report No. 109600-16-F, Environmental Research Institute of Michigan, Ann Arbor, Michigan, March 1975.

5.2 APPROACH AND PROCESSING METHODS

Most of the analysis of this Ingham County data set was carried out in last year's effort, as reported in Ref. 2. The preliminary recognition tests performed last year, and the tests carried on in this year's effort, were all made on essentially the same set of up to 50 ground-truthed training fields representing eight classes of vegetation near nadir scan angles at six different times of day from 9:33 through 14:50 LST (local solar time) (see Table 8). For each pass, one combined signature was formed from all fields for each of the eight ground covers shown in Table 9. This was reduced to six classes for purposes of calculating correct recognition by combining results for two pairs of similar crops -- (a) corn planted in two row directions and (b) pasture and hay. There were 50 fields on the first pass. In most cases the same fields and portions of fields were selected on all later passes. In a few instances, a different portion of a field was used to stay nearer nadir, and some fields were omitted either because they were too far away from nadir (the aircraft didn't repeat exactly the same flight path) or because they couldn't be reliably delineated. This cut the number of fields to 38-47 on the later passes, but we don't believe these differences had any significant effect on the results.

In last year's study, only 11-channel recognition was performed; of the 12 available channels, only channel 12 (the direct thermal radiation waveband of 9.3-11.7 μm) had been omitted because it wouldn't conform to an expected symmetry about local solar noon of the reflected radiation in the other bands. We had expected that this symmetry would lead to improving results in the afternoon, around times symmetric to the 9:33 LST signature extraction pass. However, zero correct recognition was obtained in the afternoon using 9:33 LST signatures, a fact which we have attributed to a discontinuity observed for the last two passes in the pass-to-pass calibration of channel 3 (which was not one of the channels primarily studied last year). Accordingly, channel 3 was omitted in this year's work.

TABLE 8 THE SIX PASSES MADE OVER THE INGHAM COUNTY GROUND-TRUTHED AREA ON 6 AUGUST 1971 WHICH WERE USED FOR THE RECOGNITION TESTS

	Eastern Standard Time (EST) at Middle of Pass	Local Solar Time (LST) (84.42° W Longitude)	Minutes from Local Solar Noon	Minutes Between Passes	Solar Elevation (°)
1	10:10	9:33	-147		49.3
				34	
2	10:45	10:07	-113		54.6
				48	
3	11:32	10:55	-65		60.5
				38	
4	12:10	11:33	-27		63.6
				143	
5	14:33	13:56	116		54.5
				54	
6	15:27	14:50	170		45.8

TABLE 9. INGHAM COUNTY FIELDS NEAR NADIR SCAN ANGLES WHICH WERE USED FOR THE RECOGNITION TESTS

Ground Cover	Number of Fields on First Pass	Minimum Number of Fields on Later Passes	Classes
1. Corn (planted in north-south rows)	8	6	1
2. Corn (planted in east-west rows)	12	9	
3. Pasture	5	3	2
4. Hay	8	6	
5. Trees	4	3	3
6. Oats	7	4	4
7. Dry Beans	4	4	5
8. Soybeans	2	2	6
	50	38*	

*This column sums to 37, but since the minimum number of fields occurred on different passes, the minimum number of fields per pass was 38.

Both "local" and "non-local" recognition were performed, using the ten spectral channels (see Table 10). The ERIM linear decision rule was used with its quadratic no-decision threshold test set at a threshold value for 0.001 probability of false rejection. Recognition also was repeated using only the four channels which were thoroughly studied last year (channels 1, 4, 7, and 8 at .46-.49, .52-.57, .61-.70, and .72-.92 μm, respectively).

Local recognition for each run was performed using signatures obtained by training on the entire set of fields at the same (local) time of day as the recognition test data, to serve as a standard of comparison for all non-local recognition tests. Non-local recognition always used signatures extracted from the first time of day (9:33 LST) for recognition at the remaining five times of day.

It should be noted when interpreting results that the four channels used are not necessarily the ideal subset of four channels for either local or non-local recognition, having originally been chosen merely to uniformly sample the range of wavebands. For comparison with this subset, optimum channels for local recognition were picked with program STEPL which minimizes the average pairwise probability of misclassification between signatures. Using the 9:33 LST signatures, the STEPL program picked channels in the order: 12, 8, 9, 3, 5, 6, 1, 11, 10, 4, 2, and 7. Or, omitting the thermal channel (12), the order was: 10, 4, 9, 8, 1, 6, 11, 3, 5, 2, and 7. This latter selection shows a pronounced preference for near-infrared channels, while the subset used was primarily in the visible portion of the spectrum. Neither subset is necessarily best for signature extension and non-local recognition; criteria for selecting subsets for these purposes are still the subjects of other investigations.

Non-local recognition then was repeated for the four-channel cases with new signatures obtained by multiplicatively scaling those from the first time of day to more closely match signals at the time of the recognition test data. Scaling factors were derived in three different ways and were obtained independently for each channel and for each recognition time.

TABLE 10. WAVEBANDS OF THE CHANNELS USED FOR THE RECOGNITION TESTS

Channel Number	Waveband at 10% of Peak (μm)	Previously Used For 11-Channel Recognition	Used For 10-Channel Recognition	Used For 4-Channel Recognition
1	0.46-0.49	X	X	X
2	0.48-0.51	X	X	
3	0.50-0.54	X		
4	0.52-0.57	X	X	X
5	0.54-0.60	X	X	
6	0.58-0.65	X	X	
7	0.61-0.70	X	X	X
8	0.72-0.92	X	X	X
9	1.0-1.4	X	X	
10	1.5-1.8	X	X	
11	2.0-2.6	X	X	
12	9.3-11.7			

Multiplicative scaling was chosen as being the theoretically preferred method for adjusting signatures because overall variations in illumination (total downward irradiance) were considered to be the primary cause of variations in the measured radiation, and we were specifically interested in testing how much non-local recognition could be improved with adjustments for such changes. An additive correction would have been more appropriate if path radiance variations had been predominant, but they were found to be of secondary magnitude from atmospheric radiative transfer model calculations made for these low altitudes. For each later pass, four scaling factors were found, one for each channel, and the means of all signatures from the first pass at 9:33 LST were multiplied by these factors. The covariance matrices also were scaled multiplicatively by the product of the scale factors for the two channels involved in each matrix element.

5.3 SIGNATURE ADJUSTMENTS

Three separate sets of scaling factors were derived from independent sources and used to adjust first-pass signatures. Figs. 11(a) and (b) show, as functions of time of day, the three different scaling factors used for channels 1 and 8, respectively; graphs for channels 4 and 7 (not shown) were consistent with these graphs. Note that these figures in effect show the measured or calculated illumination normalized to 1.0 on the first pass, being merely the later pass measurement divided by the corresponding first pass value.

The first adjustment method was based on the simple "cosine law" theoretical calculation that the total downward irradiance on a unit area of a horizontal plane is proportional to the cosine of the solar zenith angle (the angle between the sun and zenith) or, equivalently, to the sine of the sun's elevation angle. This can be seen to be the lowest curve on Fig. 11 (the smallest adjustment factors); note that the same curve applies for all channels. These theoretical calculations account for half or less of the variations seen in the measured radiance as represented by the top curves on the figures.

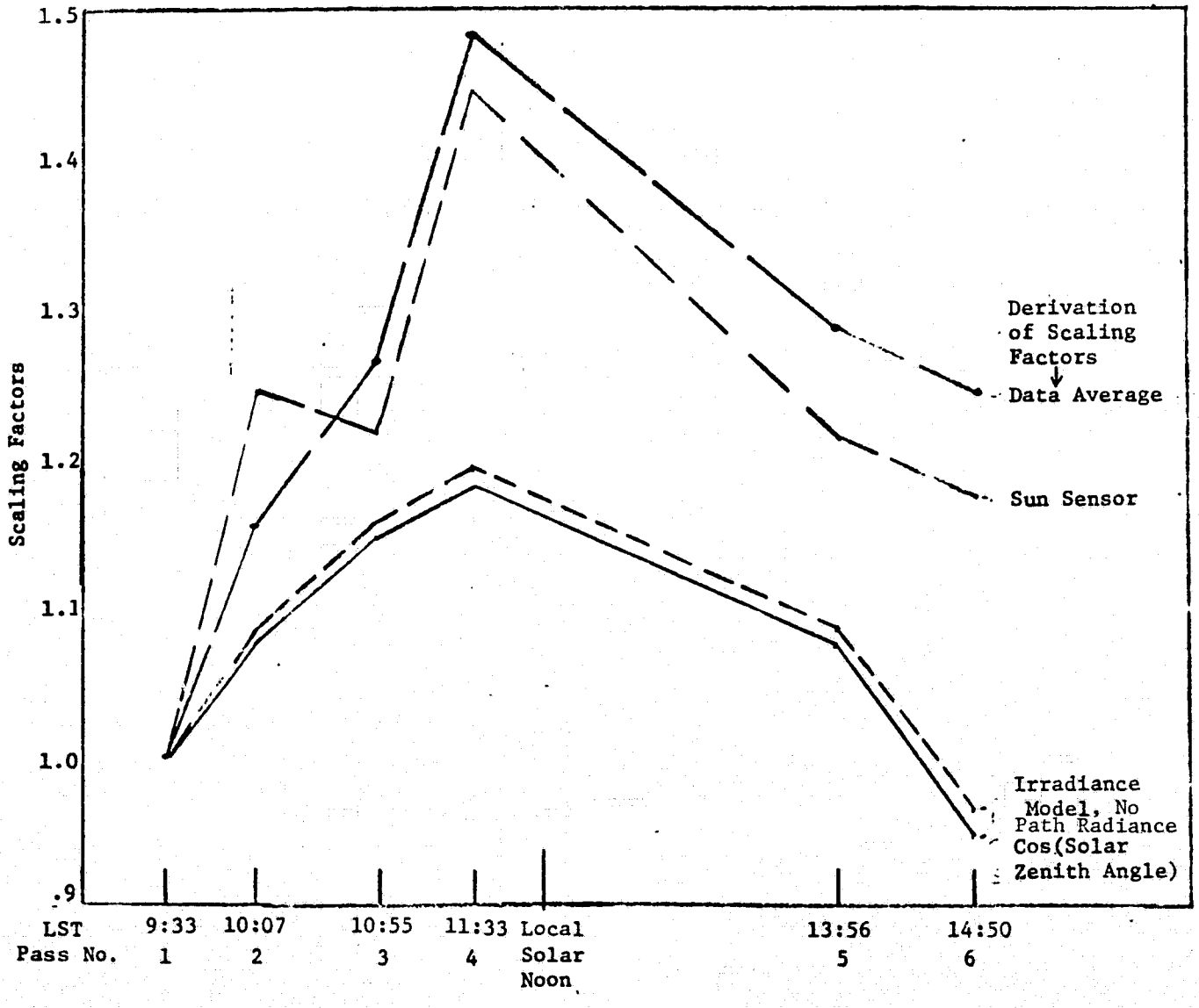

(a) CHANNEL 1 (0.46-0.49 μm)

FIGURE 11. SCALING FACTORS USED TO ADJUST FIRST-PASS SIGNATURES TO PERFORM NON-LOCAL RECOGNITION ON LATER PASSES (CONTINUED)

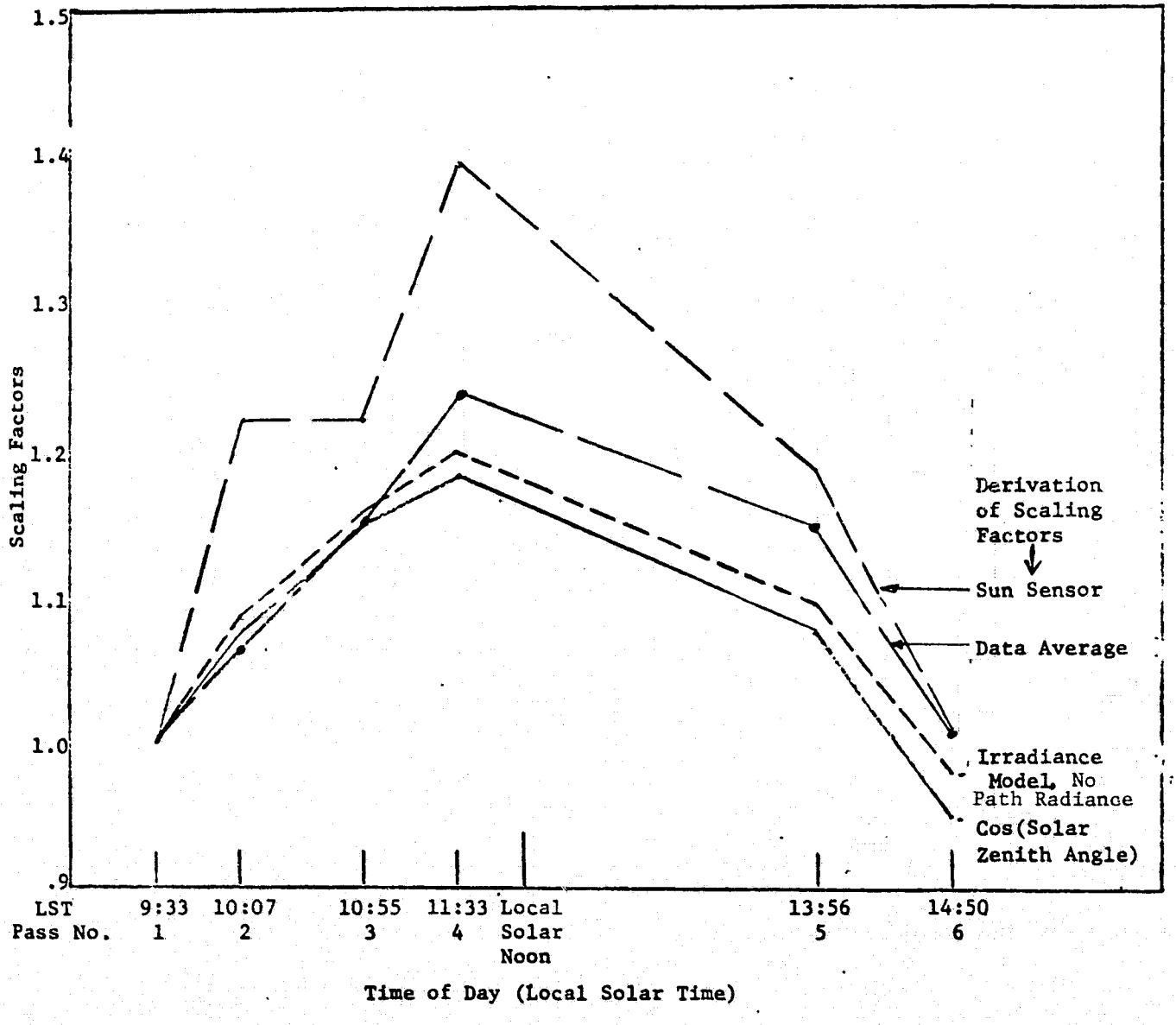

(b) CHANNEL 8 (0.72-0.92 μm)

FIGURE 11. SCALING FACTORS USED TO ADJUST FIRST-PASS SIGNATURES TO PERFORM NON-LOCAL RECOGNITION ON LATER PASSES, (CONCLUDED)

A more accurate calculation of irradiance, including atmospheric scattering, was made using a theoretical model developed by Dr. Robert Turner at ERIM [8]; assuming the 23-km visibility recorded at a nearby airport and average background reflectances, the model gave slightly higher values than did the cosine law (See Fig. 11). Although recognition tests were not made using these scale factors, they would have only modestly improved upon results with the cosine-law factors. One also could use the model to compute adjustments based on total radiance at the sensor. These adjustments should be greater than those based solely on irradiance, because they would include effects of path radiance. The value assumed for surface reflectance would be more critical for these latter calculations.

Application of either of these theoretical calculations to the data relies on the pass-to-pass consistency of the data's radiometric calibration (absolute calibration isn't needed in this case since both empirical and theoretical values effectively are normalized to the first-pass values). At least on the four channels used for the recognition tests here, thorough studies last year of the calibration failed to identify any pass to pass variations greater than about 7% at worst, but this remains a possible source of uncertainty.

The second method of adjustment was based on measurements from a sun sensor mounted on top of the aircraft to monitor the total downward irradiance at the aircraft's altitude, 1520 m (5000 ft). This method has the two advantages of (a) being able to monitor changes in illumination not accounted for by theoretical calculations (here, in particular, increased illumination scattered from the high cirrus clouds which we believe to have been present in the afternoon), and (b) being radiometrically calibrated the same as the data radiance measurements so as not to be dependent on a radiometric calibration like that needed to match data with theoretical calculations. But, this sensor has the disadvantage of two other known calibration problems -- (a) it has a non-Lambertian response (doesn't obey a cosine-law response) such that it reads too low at lower sun

---

[8] Turner, R. E., "Atmospheric Effects in Remote Sensing, Selected Papers from the March 26-28, 1973, Remote Sensing of Earth Resources Conference, Vol. II, ed. F. Shahrokhi, University of Tennessee Space Institute, Tullahoma, 1973.

elevations, and (b) it is sensitive to aircraft roll (by a cosine law, even if it were perfectly Lambertian). Because of insufficient calibration information, we decided to use sun sensor readings "as is" on the assumption that adjustments based on this sensor could nevertheless be more accurate than theoretical calculations which did not account for the presence of clouds. An average of the sun sensor readings over all scan lines on each pass was used to minimize the effect of short-term roll variations. However, between-pass variability in sun sensor readings over the first four passes, particularly, as shown on Fig. 12 indicates some problems. Despite these problems, sun sensor measurements are much closer to the average radiances from the ground than are the theoretical calculations, as can be seen on Fig. 11.

The third and final method of adjustment was based on averages of measured radiance from the ground over the entire length of each pass. The scan-angle coverage was restricted to that band of scan angles near nadir which enclosed the test fields, to avoid scan-angle-dependent variations. This method shares the two previously listed advantages of the sun-sensor method over theoretical calculations. The method also has two additional advantages over the sun-sensor method. First, it includes effects of atmospheric transmission and path radiance in the lowest portion of atmosphere (below the aircraft), the most important region as far as atmospheric effects are concerned. Second, it measures and adjusts for surface reflectance effects associated with sun angle (e.g., shadows and crop row orientation) and/or leaf attitude.

Figure 12 shows some probable effects from path radiance. At the shortest wavelength (channel 1), the scene data average gives larger adjustments than the sun sensor, but its relative magnitude diminishes progressively until it gives lower adjustments at the longest wavelength (channel 8). This trend is consistent with path radiance magnitudes which are greatest at short wavelengths; they also are greatest for situations where the scan angle is closest to the anti-solar direction (here, nearest local solar noon).

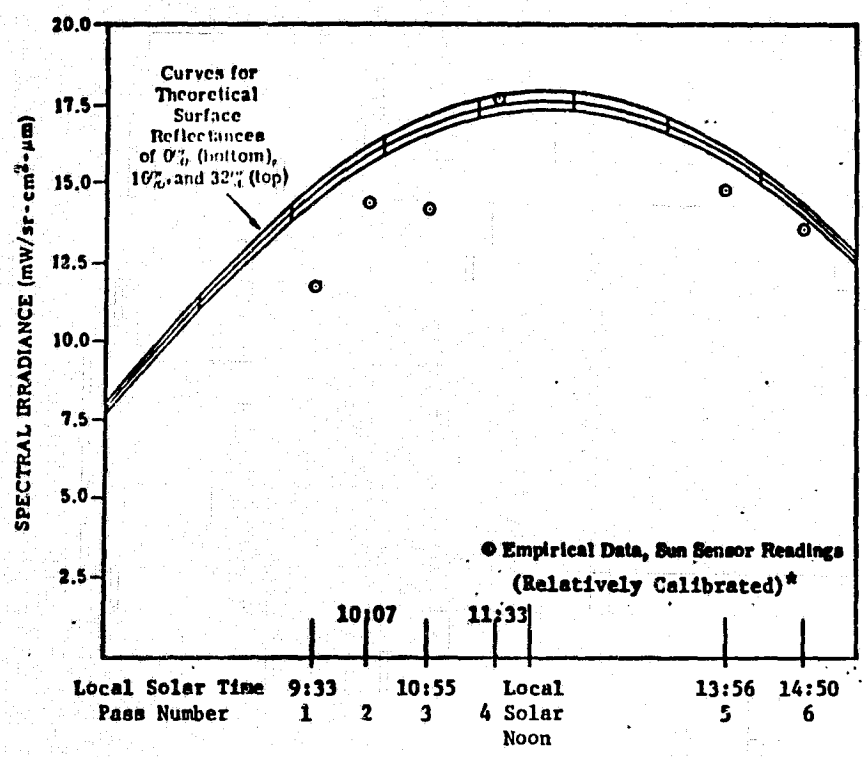

(a) Channel 1 (0.47-0.49 μm)

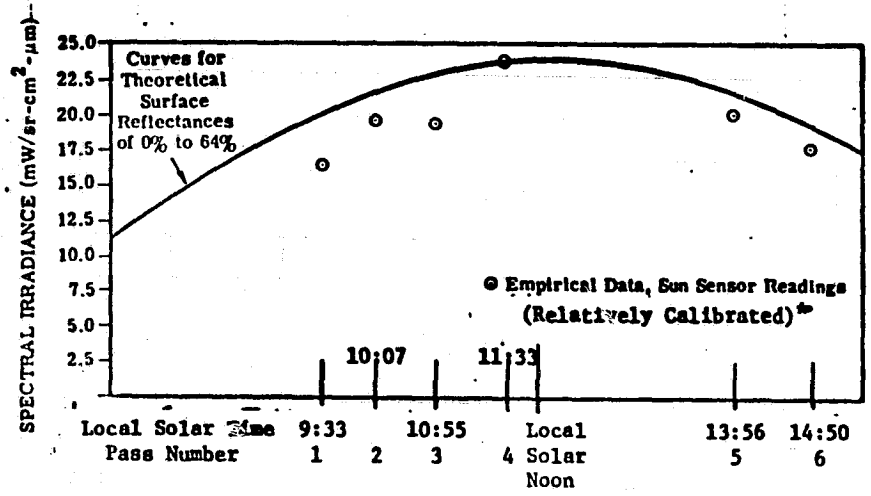

(b) Channel 8 (0.72-0.92 μm)

FIGURE 12. TYPICAL SUN-SENSOR MEASUREMENTS AT SIX TIMES OF DAY, IN COMPARISON WITH THEORETICALLY PREDICTED TOTAL DOWNWARD IRRADIANCES*

*The empirical data are relatively calibrated only, being matched to the theoretical curves near Local Solar Noon.

One potential disadvantage of the scene-data-averaging method is its dependence on the in-scene spatial distribution of both atmospheric effects and ground-cover reflectances. This potential did not materialize on this particular data set. The lower atmosphere, by all indications, was clear and unchanging during the day. Also, since essentially the same area was overflown on each pass and different cover types were randomly distributed in this predominantly agricultural data set, spatial biases were absent or minimal. As a check of uniformity and consistency with the ground covers of interest, the ground data averages also were calculated using the average over signature means for all classes, giving very similar results for both the scaling factors and the subsequent recognition. Yet, as reported last year [2], there were notable differences between means of the various ground cover classes at nadir.

5.4 RECOGNITION RESULTS

As one indicator of success, correct recognition percentages for the six cover types were averaged over the last five passes. These averages are presented in Table 11, with breakdowns by time of day being given in Figs. 13 and 14.

Local recognition with ten channels averaged 88.8% correct which is similar to the 11-channel results obtained last year.* Four-channel results averaged 78.3% which is still a reasonable performance level. The figures show that local recognition was quite consistent over all six passes.

---

[2] Malila, W. A., R. H. Hieber, and J. E. Sarno, "Analysis of Multispectral Signatures and Investigation of Multi-Aspect Remote Sensing Techniques", Report No. NASA CR-ERIM 109100-27-T, Environmental Research Institute of Michigan, Ann Arbor, Michigan, July 1974.

*These results are not exactly comparable to the 11-channel recognition results reported last year since slightly different methods of averaging were used which can cause differences of a few percent. Last year's averages were weighted by the number of pixels in the field. Since we believed this put too much emphasis on the larger fields, all class averages in this report are for fields weighted uniformly within a cover class, and uniform weighting of classes was used to get the average over classes.

TABLE 11. RECOGNITION ACCURACIES AVERAGED OVER THE LAST FIVE TIMES OF DAY USED FOR THE NON-LOCAL RECOGNITION TESTS

Signatures Used	Average Percent Correct: 10 Channel Recognition	Average Percent Correct: 4 Channel Recognition
Extracted at Same Time (Local Recognition)	88.5%	78.3%
Extracted from First Time of Day,		
Unmodified	11.1%	16.3
Scaled by Cos(Sun Zenith Angle)	N/A	40.7
Scaled by Sun and Sky Sensor	N/A	62.0
Scaled by Center Data Average	N/A	74.1

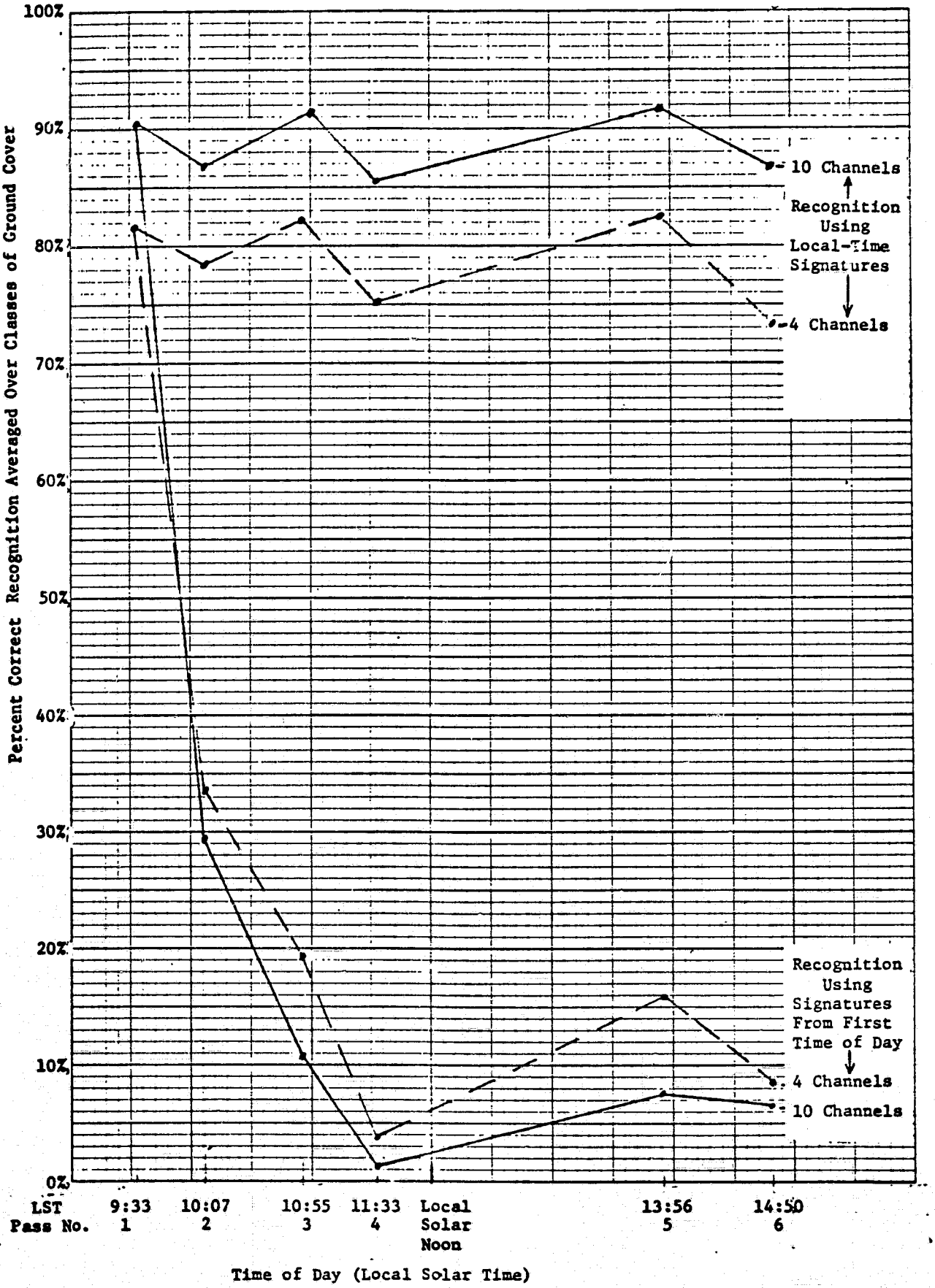

FIGURE 13. RESULTS FOR LOCAL RECOGNITION AND FOR NON-LOCAL RECOGNITION WITH NON-ADJUSTED FIRST-PASS SIGNATURES AT SIX TIMES OF DAY -- USING 4 and 10 CHANNELS

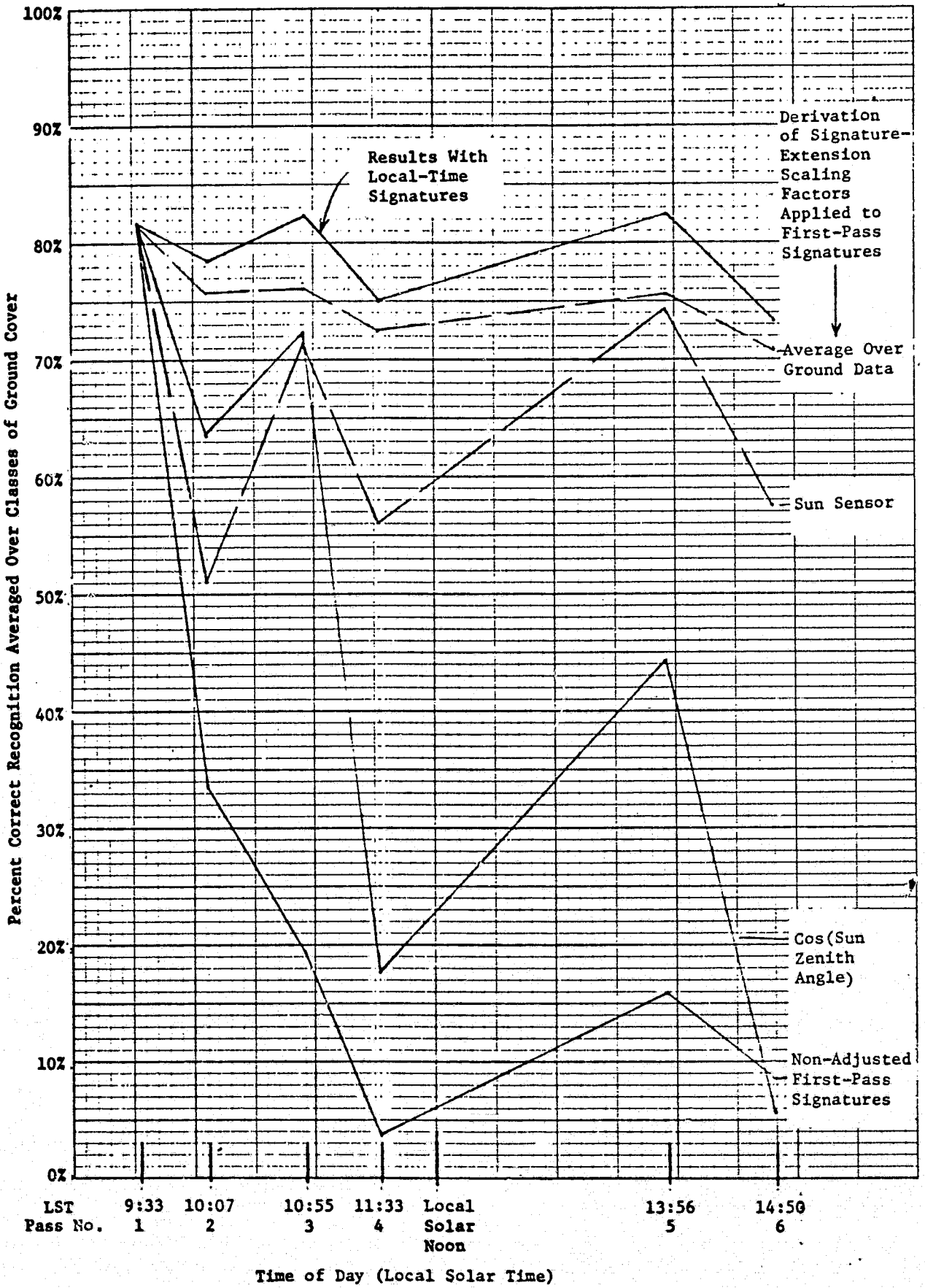

FIGURE 14. RESULTS FOR RECOGNITION AT SIX TIMES OF DAY USING 4 CHANNELS WITH VARIOUS ADJUSTMENTS OF FIRST-PASS SIGNATURES TO COMPENSATE FOR VARYING ILLUMINATION

The major difference between non-local recognition results this year and last, with non-adjusted first-pass signatures, is the finite recognition percentage obtained for the two afternoon runs this year in contrast with the zero percentages obtained last year. Also, while the percentages for the noon run this year dipped to 1.2% and 3.9% correct for ten and four channels, respectively, they rose again in the afternoon as the sun's zenith more closely matched its value for the first pass. The afternoon rises (to only 6-16%) were not as great as would be expected, based only on the sun's zenith angles for the passes. We believe, as discussed earlier, that changes in illumination conditions in the afternoon (due to high thin cirrus clouds) were the predominant factors in this degradation.

Another fact evident on Fig. 13 is that non-local recognition is better with four channels than with ten. This difference could be due to undetected pass-to-pass calibration variations in one of the six channels not included in the subset of four. Another, perhaps more likely, reason is that there are more ways to deviate from original conditions in the signal space of ten channels than in that of four. This result tends to corroborate results of another study [11] which found that a fewer number of channels was better for signature extension.

Non-local recognition results were improved substantially by multiplicative scaling adjustments made on first-pass signatures prior to four-channel non-local recognition tests. As contrasted to the average 16.3% correct recognition over the last five passes with non-adjusted signatures, the cosine (of the sun zenith angle) adjustment gave 40.7% average correct recognition. However, pass-to-pass fluctuations in the accuracy were quite erratic, as shown on Fig. 14, possibly due to radiometric calibration

---

[11] Vincent, R., G. Thomas, and R. Nalepka, "Signature Extension Studies", Report No. 190100-26-T, Environmental Research Institute of Michigan, Ann Arbor, Michigan, July 1974.

discrepancies. The poorer results in the afternoon are consistent with our hypothesis that clouds increased the irradiance then.

Recognition accuracy increased to an average of 62% correct with signatures adjusted according to sun-sensor readings and, in particular, maintained this level of accuracy for the afternoon passes. The pass-to-pass variation is still sizeable but is much reduced from that of the cosine-law and is relatively the same in both morning and afternoon, presumably being affected by the sun sensor's own calibration (though no longer dependent on the scanner's radiometric calibration).

Finally, when signature adjustments were made according to scene averages, recognition results were very good, being 74.1% correct on the average (only 4.2% lower than local recognition accuracy averaged over the same last five passes). Further, the results are quite consistent, being only 2.3% to 6.8% less accurate than the corresponding local recognition accuracies and more consistent than the local recognition results. Fig. 14 illustrates that the recognition accuracy for the scene-signal-averaging method of adjustment is better and more consistent at all times than the other two adjustment methods.

The success of the last adjustment approach demonstrates that, given a sufficiently good determination of the average variation in radiation, it is possible to correct reasonably well for large variations in one primary parameter, irradiation in this case (with sun angle and bidirectional effects contributing possible secondary effects). It was by no means obvious a priori that one correction factor (for each channel) would suffice to satisfactorily correct not only the means of signatures for six classes of vegetation, but also the covariance matrices. At worst, one factor per channel might be able to properly adjust the means of only one signature at a time (and not necessarily its covariance matrix).

5.5 CONCLUSIONS AND RECOMMENDATIONS

Changes in multispectral scanner data throughout a day are substantial and can cause severe degradation in recognition performance. Correction methods do exist which can compensate for these changes and maintain high levels of recognition performance. Of the three methods tested, signature adjustments based on average signals over the scene proved to be the best, while those based only on theoretical sun angle corrections were the poorest (although they did offer some improvement over unadjusted signatures).

Although not of major relevance to the specific study reported, it is of interest to make the following observations. Average local recognition performance with a subset of four channels was ten percentage points lower than with ten non-thermal channels; however, the optimum subset was not used. Calculations of optimum channels, based on average pairwise probability of misclassification, showed that the preferred channel was the thermal, followed by two near infrared and then a visible channel. When the thermal channel was excluded, near-infrared channels were chosen first, third, and fourth, with a visible channel being chosen second.

REFERENCES

1. Malila, W.A., D.P. Rice, and R.C. Cicone, "Final Report on the CITARS Effort by the Environmental Research Institute of Michigan", Report No. NASA CR ERIM 109600-12-F, E.R.I.M., Ann Arbor, Michigan, 2/75.

2. Malila, W.A., R.H. Hieber, and J.E. Sarno, "Analysis of Multispectral Signatures and Investigation of Multi-Aspect Remote Sensing Techniques", Report NASA CR ERIM 109100-27-T, E.R.I.M., Ann Arbor, Michigan 7/74.

3. Crane, R.B., and W. Richardson, "Performance Evaluation of Multispectral Scanner Classification Methods", Proceedings of the 8th International Symposium on Remote Sensing of Environment, Vol. II, Report No. 195600-1-X, E.R.I.M., Ann Arbor, Michigan 1972, pp. 815-31.

4. Nalepka, R.F., H.M. Horwitz, and P.D. Hyde, "Estimating Proportions of Objects from Multispectral Data", Report NASA CR WRL 31650-73-T, Willow Run Laboratories, University of Michigan, Ann Arbor, Michigan 3/72.

5. Suits, Gwynn H., 1972. "The Calculation of the Directional Reflectance of a Vegetative Canopy", Remote Sensing of Environment, Vol. 2, pp. 117-125.

6. Safir, G.R., G.H. Suits, and M.V. Weiss, 1972. "Applications of a Directional Reflectance Model to Wheat Canopies Under Stress", Proceedings of International Conference on Remote Sensing in Arid Lands, Tuscon, Arizona, Nov. 9, 1972.

7. Wiegand, C.L., et.al., 1971. Spectral Survey of Irrigated Region Crops and Soils, 1971 Annual Report, Weslaco Agricultural Research Center, U.S. Department of Agriculture, Weslaco, Texas, December 1971.

8. Turner, R.E., "Atmospheric Effects in Remote Sensing, Selected Papers from the March 26-28, 1973, Remote Sensing of Earth Resources Conference, Vol. II, ed. F. Shahrokhi, Univ of Tennessee Space Institute, Tullahoma, 1973.

9. Turner, R.E., W.A. Malila, R.F. Nalepka, and F.J. Thomson, "Influence of the Atmosphere on Remotely Sensed Data", Proceedings of SPIE Seminar on Scanners and Imagery Systems for Earth Observation, August 1974.

10. Horwitz, H., J. Lewis, and A. Pentland, "Estimating Proportions of Objects from Multispectral Scanner Data", Report No. 109600-13-F, Environmental Research Institute of Michigan, Ann Arbor, Michigan, March 1975.

REFERENCES (Cont'd)

11. Vincent, R., G. Thomas, and R. Nalepka, "Signature Extension Studies", Report No. 190100-26-T, Environmental Research Institute of Michigan, Ann Arbor, Michigan, July 1974.

12. Henderson, R. G., G. S. Thomas, and R. F. Nalepka, "Methods of Extending Signatures and Training Without Ground Information", Report No. 109600-16-F, Environmental Research Institute of Michigan, Ann Arbor, Michigan, March 1975.